

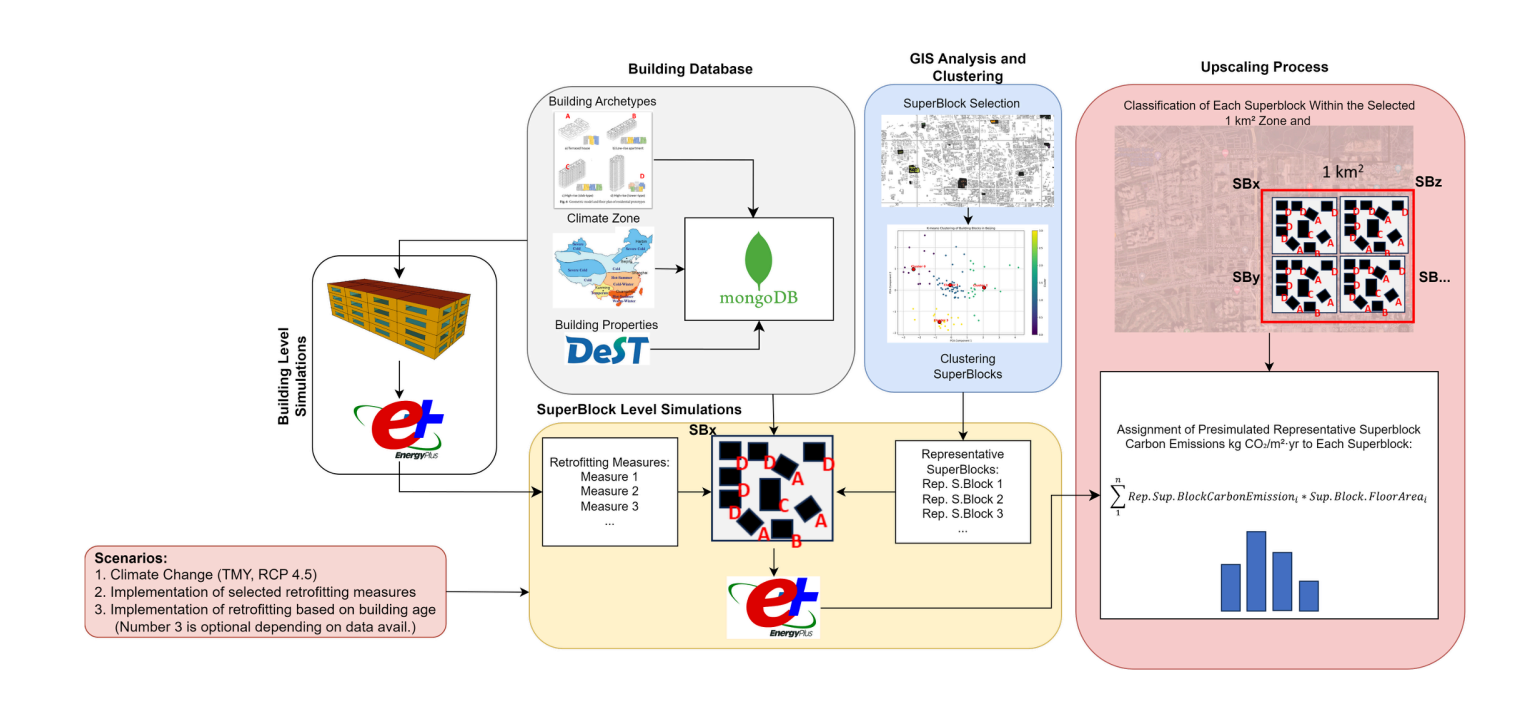


Sino-Swiss Cooperation on Zero Emissions Building

Technical Report

Impact Simulation of the Chinese ZEB Standard

ENGLISH VERSION



MARCH 2025









This report has been produced within the framework Sino-Swiss Zero Emissions Building Project; an international collaboration funded by the Swiss Agency for Development and Cooperation in partnership with the Chinese Ministry of Housing and Urban-Rural Development.

Authors:

Sadik, Yigit, ZHAW IBP, sadik.yigit@zhaw.ch Juan, Mahecha, ZHAW IBP, mahe@zhaw.ch Luca, Baldini, ZHAW IBP, luca.baldini@zhaw.ch

Subsidy recipients:

ZHAW Institute for Building Technology and Process IBP. Tössfeldstrasse 11, 8401 Winterthur https://www.zhaw.ch/de/archbau/institute/ibp



Cite as:

Yigit, S., Mahecha, J., Baldini, L. (2025). Impact Simulation of the Chinese ZEB Standard. Sino-Swiss Zero Emissions Building Project Research Report. Intep-Skat: Zurich

The Sino-Swiss Zero Emissions Building Project is an international collaboration funded by the Swiss Agency for Development Cooperation in partnership with the Chinese Ministry of Housing and Urban-Rural Development. The project aims to reduce greenhouse gas emissions and enable carbon neural development of the building sector in China by sharing Swiss know-how on sustainable and zero emission building.

Implementation partners:

Intep Integrated Planning
Skat Consulting
China Academy of Building Research

WeChat: SinoSwissZEB



Web: zeb-china.org



Cover image: ©ZHAW, 2025

Summary

The transition to zero-emission buildings is crucial for significantly contributing to China's low-emission goals. This research quantifies the impact of newly introduced zero-carbon building standards on emission reduction targets across various urban areas. Focusing on four representative climate zones—hot summer and warm winter (Shenzhen), extremely cold (Harbin), cold (Beijing), and hot summer and cold winter (Shanghai)—the study proposes a GIS-based methodology to assess the emission outcomes of implementing zero-carbon building standards in residential buildings.

Each building in the existing stock is categorized into an archetype (terraced house, low-rise, high-rise slab, or high-rise tower) based on its height and typology. Once the archetype is identified, the corresponding envelope configuration and operation schedules taken from the DeST database and literature are assigned to simulate the baseline heating and cooling energy demands. Simulation results indicate significant variations in energy performance based on climate region, building age, and archetype. Older buildings and terraced houses, demonstrate higher specific energy demands, particularly in heating-dominated regions like Beijing and Harbin, where baseline carbon emissions range from 31.3 to 74.2 kg CO₂eq/m²/y and 37.1 to 79.4 kg CO₂eq/m²/y, respectively. In contrast, emissions in cooling-dominated regions like Shenzhen range from 38.2 to 42.0 kg CO₂eq/m²/y, while more balanced climates like Shanghai exhibit values between 45.0 and 59.3 kg CO₂eq/m²/y.

Retrofit strategies were evaluated for each climate region, revealing that envelope upgrades (e.g., insulation and window improvements) are highly effective in heating-dominated regions. In contrast, HVAC and PV system improvements yield the highest benefits in both cooling- and heating-dominated regions, while a combination of measures proves most effective in balanced climates. Electrification through heat pumps and PV integration further enhances emission reductions, with net-negative emissions achievable in low-rise buildings and areas with sufficient solar potential.

To extend the analysis, results were upscaled to larger urban areas by selecting representative superblocks using k-means clustering. This clustering, based on key characteristics such as U-factor, shape factor, and density, enabled the identification of distinct superblock typologies. The study calculated total carbon reduction potential across all upscaling zones, showing annual emissions reductions of 68,100 tons CO_2 eq/yr (Beijing), 73,606 tons CO_2 eq/yr (Harbin), 73,296 tons CO_2 eq/yr (Shanghai), and 118,390 tons CO_2 eq/yr (Shenzhen) under current grid carbon intensity conditions.

By classifying superblocks within multiple zones of approximately 1 km² each, the study provides a broader assessment of energy consumption and carbon emissions at the urban scale. This superblock-level approach enhances energy performance assessments by accounting for shading effects from neighbouring buildings, improving the upscaling capability and accuracy of retrofit strategies. The framework effectively identifies priority zones for retrofits, particularly older, low-rise buildings and superblocks with high shape factors, which exhibit the highest energy demands.

Ultimately, this study provides valuable insights for policymakers, urban planners, and designers, supporting the transition to low-emission urban development and aligning with global climate goals. However, the findings also underscore the importance of data quality and availability, as accurate and comprehensive datasets are essential for optimizing the performance of the proposed framework. By demonstrating the potential of zero-carbon standards at both building and urban scales, this research contributes to China's efforts to achieve a zero-emission future.

Main findings («Take-Home Messages»)

- This study offers valuable insights for policymakers, urban planners, and designers in China, aiding the country's transition to low-carbon urban development while contributing to global climate goals.
- This methodology establishes a replicable framework for assessing the urban-scale impact of zerocarbon building standards, providing policymakers with actionable data to support strategic planning and decarbonization efforts.
- The energy performance of residential buildings in China varies significantly by climate region, age, and archetype, with older buildings and certain archetypes, such as terraced houses, showing higher specific energy demands, especially in heating-dominated regions.
- Effective retrofit strategies strongly depend on the climate: envelope upgrades are effective in heating-dominated regions, HVAC and PV system improvements are highly effective in both coolingdominated and heating-dominated regions, and a combination of measures is effective in balanced climates.
- The results demonstrate that decarbonization of the electricity grid is essential. With a 25% reduction in the grid's carbon emission intensity to 0.5126 kgCO₂eq/kWh, all superblocks meet the nearly zero-carbon emission thresholds defined in the new Zero-Carbon Building Standard under Scenario 3, in which both passive and active measures are applied to buildings.
- The study demonstrates that superblock-level analysis makes energy performance assessments more realistic compared to pure building-level analysis, by accounting for shading effects from neighbouring buildings. It also improves the upscaling capability and accuracy of retrofit strategies, ensuring more effective planning and implementation.
- The effectiveness of the proposed framework strongly depends on the quality and availability of data, highlighting the need for more accurate and comprehensive datasets on China's building stock. In this study, data for key parameters such as building height, construction year, footprint, and superblock characteristics were especially important.

Contents

Sumr	mary		3								
Main	findings	(«Take-Home Messages»)	4								
Conte	ents		5								
List c	of figures	·	е								
List c	of tables.		7								
List c	of abbrev	riations	8								
1	Introd	uction	9								
1.1.	Backg	round	9								
1.2.	Purpos	se of the project	10								
1.3.	Projec	t objectives	10								
2	Appro	ach, method, results and discussion	1 1								
2.1.	Work	Work package A - case study selection									
	2.1.1.	Climatic diversity	12								
	2.1.2.	3.1 ° 63									
	2.1.3.	Data availability	13								
2.2		package B - establishing a baseline for building archetypes									
	2.2.1.	Development of building models	15								
	2.2.2.	Results of the analysis	16								
2.3	Work p	package C - impact modelling of ZEB for archetype buildings									
	2.3.1.	, , ,									
	2.3.2.	Decarbonization pathways	19								
	2.3.3.	Carbon emission calculations	20								
	2.3.4.	The results of the analysis	21								
2.4	Work p	package D - superblock analysis	23								
	2.4.1.										
	2.4.2.	Baseline and scenario analysis	32								
2.5	Work F	Package E and Work Package F– Upscaling Process and Scenario Analysis	37								
	2.5.1.	Beijing – Upscaling	37								
	2.5.2.	Harbin – upscaling	40								
	2.5.3.	Shanghai – upscaling	42								
	2.5.4.	Shenzhen – upscaling	44								
3		usions									
4		ok									
5	Public	ations and other communications	49								
6	Dofore	2000	40								

List of figures

Figure 1: General Framework of the Implemented Approach	11
Figure 2: Climate Region Distribution in China (Dai et al., 2022).	13
Figure 3: The process of translating and merging DeST database into MongoDB	15
Figure 4: Schedules for Occupancy, Lighting, and Appliances	16
Figure 5: Comparison of EnergyPlus and DeST simulation results for Beijing 2010-2018	17
Figure 6: Results of the Baseline Simulations	17
Figure 7: EnergyPlus/CESAR-P Archetype configuration – Building level	18
Figure 8: General framework for superblock level analysis	23
Figure 9: Superblock selection process	24
Figure 10: Completing missing data for building footprints	24
Figure 11: Simple statistics of selected superblocks	25
Figure 12: Clustering analysis with principal component visualization	27
Figure 13: Exploratory statistical analysis for clusters	28
Figure 14: Representative clusters for Beijing	29
Figure 15: Representative clusters for Harbin	30
Figure 16: Representative clusters for Shanghai	31
Figure 17: Representative clusters for Shenzhen	32
Figure 18: Selected upscaling zone for Beijing	38
Figure 19: Beijing superblock clusters for upscaling zone	39
Figure 20: Selected upscaling zone for Harbin	40
Figure 21: Harbin superblock clusters for upscaling zone	41
Figure 22: Selected upscaling zone for Shanghai	42
Figure 23: Shanghai superblock clusters for upscaling zone	43
Figure 24: Selected upscaling zone for Shenzhen	44
Figure 25: Shenzhen Superblock Clusters for Upscaling Zone	45

List of tables

Table 1: The geometrical information and natural ventilation rates for building archetypes	14
Table 2: HVAC systems for the current and retrofitted design of the buildings	19
Table 3: Decarbonization pathways determined for energy performance improvement	20
Table 4: Nearly zero carbon residential building carbon dioxide emission intensity (kgCO ₂ eq/m ² y)	20
Table 5: Simulation results of the building level analysis under defined measures, considering HVA and DHW systems (kgCO₂eq/m²y)	C 21
Table 6: Simulation results of the building-level analysis under measures including emissions from electric appliances and lighting (kgCO₂eq/m²y)	22
Table 7: Decarbonization Pathways Determined for Energy Performance Improvement	. 33
Table 8: Results of the representative superblock analysis under defined scenarios, excluding elect appliances and lighting (kg CO₂eq/m²·y)	
Table 9: Results of the representative superblock analysis under defined scenarios including electri appliances and lighting (kg CO₂eq/m².y)	
Table 10: Results of the representative superblock analysis under defined scenarios, including elecappliances and lighting, with a 25% decarbonized electricity grid (kg CO₂eq/m².y)	
Table 11: Results of the representative superblock analysis under defined scenarios, including elecappliances and lighting, with a 50% decarbonized electricity grid (kg CO₂eq/m².y)	
Table 12: Results of the representative superblock analysis under defined scenarios, including elecappliances and lighting, with a 90% decarbonized electricity grid (kg CO₂eq/m².y)	
Table 13: Beijing carbon emissions for upscaling zone (kg CO₂eq/m².y)	. 39
Table 14: Harbin Carbon Emissions for Upscaling Zone (kg CO ₂ eq/m².y)	. 41
Table 15: Shanghai Carbon Emissions for Upscaling Zone (kg CO₂eq/m².y)	. 43
Table 16: Shenzhen Carbon Emissions for Upscaling Zone (kg CO₂eq/m².y)	. 45

List of abbreviations

- ACH: Air Changes per HourASHP: Air Source Heat Pump
- CABR: China Academy of Building Research
- CESAR-P: Comprehensive Energy System Analysis and Retrofit Planning
- DeST: DeST (Designer's Simulation Toolkit)
- DHW: Domestic Hot Water
- **GB/T:** Guobiao Standards (Chinese National Standards)
- GIS: Geographic Information System
- **HP**: Heat Pump
- HVAC: Heating, Ventilation, and Air Conditioning
- MoHURD: Ministry of Housing and Urban-Rural Development
- NZEB: Nearly Zero Energy Building
- **PV**: Photovoltaic
- SHGC: Solar Heat Gain CoefficientSSP: Shared Socio-economic Pathway
- U-factor: Thermal Transmittance
- WP: Work Package
- ZEB: Zero Emission Building

1 Introduction

1.1. Background

China is the top CO₂-emitting country in the world (X. Ma et al., 2019) and has set carbon reduction goals, aiming to peak carbon emissions by 2030 and achieve carbon neutrality by 2060 (J. Wang et al., 2021). The building energy consumption in China accounts for roughly a third of the total energy demand and dynamically changes due to factors such as floor space, income, and population (Yu et al., 2014). For this reason, the transition to zero-carbon buildings is essential to mitigate climate change, particularly in regions with rapidly expanding urban environments. A large-scale ascending of zero-emission buildings (ZEBs) is required to reduce emissions (Yang et al., 2019), where energy demand reduction can be successfully achieved through various measures and technological advancements. Building energy performance depends largely on physical building properties, which can be improved through retrofits guided by stricter building standards. Thus, implementing zero emission building regulations is a key strategy in aligning urban development with national climate targets.

Prior studies have emphasized the key role of building energy efficiency in mitigating emissions. Research on Shenzhen which is a major economic hub in China has shown that operational emissions from buildings nearly doubled between 2005 and 2019 (J. Wang et al., 2021). Studies indicate that strict energy efficiency policies and renewable energy integration could allow the building sector to peak emissions by 2025, five years ahead of China's national target. Ma et al. (2020) investigated historical carbon mitigation efforts and projected emission peaks, highlighting the need for enhanced policy frameworks, financial incentives, and technological advancements. Geng et al. (2022) further quantified carbon emissions from urban residential buildings in the Greater Bay Area (Guangdong–Hong Kong–Macao), identifying operational emissions as the dominant factor in total carbon output.

Furthermore, previous research has explored the role of energy conservation and generation measures such as envelope upgrades, daylight optimization, and photovoltaic system integration in reducing carbon emissions. Advanced energy modelling tools, such as AutoBPS (Deng et al., 2023), have been developed to simulate energy demand, assess shading impacts, and evaluate retrofitting strategies for improved efficiency. Li and Wong (2007) analysed the implications of shading effects from nearby buildings on energy consumption and daylighting. The applicability of different measures such as efficient thermal insulation systems, high-performance window systems, good airtightness, and fresh air heat recovery systems have been examined in the Chinese context (Z. Liu et al., 2019). Braun et al. (2012) explored large-scale photovoltaic deployment and its impact on distribution grids, highlighting the technical and regulatory challenges associated with high PV penetration. Studies by Valencia et al. (2022) and Shea et al. (2020) have examined carbon-neutral building environments and energy-efficient retrofits at a city scale, underlining the importance of urban planning in achieving long-term emission reduction goals.

Other research efforts have examined the role of on-site electricity generation and energy storage in achieving carbon neutrality. Wiryadinata et al. (2019) and Opel et al. (2017) emphasize the importance of integrating heat pumps and combined heat and power systems with low-temperature renewable energy sources like solar and geothermal. The economic feasibility of zero-carbon transition has also been analysed, with studies suggesting that policy interventions and financial incentives are essential to drive large-scale adoption (Huang et al., 2022). Moreover, Deng et al. (2023) highlight the importance of urban-scale energy modelling for supporting city-wide energy efficiency strategies. Various methodologies have been used to estimate and project China's building energy demand, including Global Assessment Models (Eom et al., 2012) and the China Building Energy Model Guo et al. (2021). Studies on zero-energy buildings have explored aggregated-level implications, albeit without incorporating a spatial GIS dimension (Yang et al., 2019; S.-C. Zhang et al., 2021). For representative building stock analysis, existing work by An et al. (2023) serves as a strong foundation.

1.2. Purpose of the project

While numerous studies have assessed the effectiveness of mitigation strategies such as building envelope improvements, HVAC system changes, renewable energy integration, and smart controls, significant challenges persist in modelling these interventions across spatiotemporal scales. This is particularly evident when extrapolating energy-saving potential to regional or national levels (Eggimann et al., 2022). A holistic approach that integrates spatial modelling with energy simulation techniques is critical to systematically evaluate building retrofits at broader scales.

This study quantifies the impact of zero-carbon building standards across diverse urban climates in China. By using a GIS-based methodology, the research evaluates the emission reduction outcomes of implementing these standards in residential buildings. Buildings are grouped into archetypes based on height and age, with corresponding envelope configurations and occupancy schedules assigned to each category. Simulations of baseline heating and cooling energy demands are then conducted, offering insights into achievable energy savings and emissions reductions under zero-carbon standards.

The key barrier to scaling zero-carbon solutions is the increased complexity of applying them from individual buildings to entire urban districts (Keirstead et al., 2012). To address this, the study upscales building-level data through k-means clustering, identifying representative urban "superblocks." These superblocks serve as reference points for categorizing wider urban zones, enabling city-level estimations of energy use and emissions. Superblocks are synonymous with street blocks and often represent a real estate area developed simultaneously. In Chinese cities, superblocks form a predominant urban pattern and are therefore considered an appropriate unit for urban energy performance analysis and upscaling (Johnson et al., 2022). This methodology establishes a replicable framework for assessing the urban-scale impact of zero-carbon standards, empowering policymakers with actionable data for strategic planning.

By combining energy modelling with urban-scale analysis, this research systematically evaluates the feasibility and efficiency of zero-carbon building standards across Chinese cities. The findings advance an understanding of how such strategies can align with national and global decarbonization goals while contributing actionable recommendations for optimizing energy efficiency in rapidly urbanizing regions. Ultimately, the study supports sustainable urban development discussion by offering scalable pathways to mitigate building-sector emissions.

1.3. Project objectives

In this research, the following research questions are addressed:

- What is the energy performance of the current stock of residential buildings in different cities / climate regions of China?
- How does the new zero-emission standard affect emissions across diverse urban climates in China?
- Which retrofit strategies (e.g., envelope upgrades, HVAC improvements, etc.) offer the most effective/impactful reductions in emissions for specific climatic zones?
- Can the proposed framework identify priority zones (e.g., high-emission/low-performance superblocks) for targeted retrofits, thus guiding policymakers' resource allocation?

Answering the above questions translates into the following main goals:

- Assessing the energy performance of existing residential buildings: Evaluating the current energy demand of buildings across different cities and climate zones in China to establish a baseline for energy efficiency and emission reduction potential.
- Quantifying the impact of Zero-Carbon Standards: Investigating how the implementation of zero-carbon building standards influences heating and cooling energy demands across China's diverse urban climates.
- Identifying effective retrofit strategies: Comparing the impact of various retrofit measures, such as envelope and HVAC upgrades, to determine the most suitable strategies for specific climatic zones.
- Identifying prioritized zones for retrofitting: The proposed framework helps authorities identify
 the zones with the highest impact on carbon emissions, which should be prioritized for retrofitting.
- Comparing Simulation Scales: Analysing how energy and carbon reduction outcomes differ between superblock-level and individual building-level simulations.

2 Approach, method, results and discussion

This project employs a comprehensive methodology to analyse individual buildings and superblocks, upscaling the results to larger zones of 1 km². The framework, illustrated in Figure 1, is structured into three levels: Building Level, Superblock Level, and Upscaling to Larger Zones.

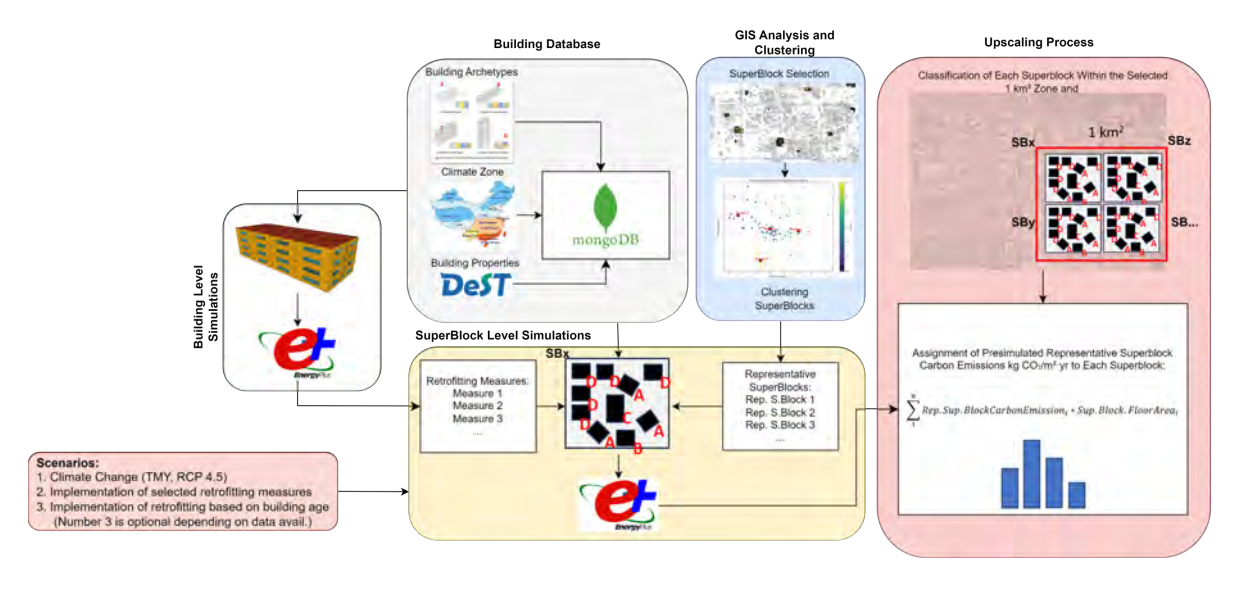


Figure 1: General Framework of the Implemented Approach.

At the Building Level, building archetypes and models are sourced from established databases. A Python script extracts relevant data (e.g., geometry, materials, schedules) for EnergyPlus simulations, considering building type, age, and climate region. Key parameters such as occupancy schedules, thermostat setpoints, and equipment usage are derived from the DeST database, NZEB standard and literature (An et al., 2023; Housing & China (MoHURD), 2019). The Cesar-P tool, powered by EnergyPlus, simulating archetypes, and retrofitting measures is applied to evaluate performance improvements. The results guide the superblock-level scenario analysis (Orehounig et al., 2022).

At the Superblock Level, building archetypes are categorized and clustered using the k-means method to identify common patterns. Representative superblocks are selected for each cluster and simulated under various scenarios, including climate change, to assess their energy performance and carbon emissions.

Finally, the Upscaling process applies the superblock results to zones of approximately 1 km² in size, for selected cities. Different scenarios are analysed to evaluate their impact on energy performance and carbon emissions. Retrofit levels are also examined to assess potential improvements.

The project is organized into six work packages:

- A: Case study definition and data collection
- B: Evaluation of the baseline performance for building archetypes
- C: Impact modelling of ZEB for archetype buildings
- D: Superblock analysis
- E: Upscaling to 1 km² areas
- F: Scenario analysis

Detailed explanations for each step are provided in the following sections 2.1 to 2.5.

2.1. Work package A - case study selection

The selection of Beijing, Harbin, Shenzhen, and Shanghai as case study cities for analysing the transition to zero-carbon buildings is grounded in their distinctive characteristics, climate diversity, and role in China's broader low-carbon policy initiatives. These cities represent varied geographical and climatic zones, reflecting China's diverse urbanization and development patterns. Beijing, Shenzhen, and Shanghai are key participants in China's low-carbon city pilot policy, with Shenzhen (first batch, 2010) leading in green innovation, and Beijing and Shanghai (second batch, 2012) focusing on energy-efficient buildings, public transport, and carbon trading (Zhou & Zhou, 2021). While not part of the pilot, Harbin provides valuable insights due to its colder climate, enriching the analysis of zero-carbon transitions across diverse contexts.

2.1.1.Climatic diversity

The selected cities incorporate a wide range of climates in China, which allows for a comprehensive analysis of how climate impacts the energy performance and retrofit potential of buildings (Dai et al., 2022; H. Wang et al., 2015). As it can be seen from Figure 2. China is divided into 5 climate regions. Beijing represents northern China with cold winters and hot summers, demanding heating and cooling solutions. Harbin, located in northeastern China, has a frigid climate, offering a unique opportunity to study heating demands in cold regions. Shenzhen, located in southern China, experiences a tropical climate that emphasizes cooling needs. Shanghai combines a humid subtropical climate, with significant seasonal variation in heating and cooling requirements, making it a key representative of coastal cities.



Figure 2: Climate Region Distribution in China (Dai et al., 2022).

2.1.2. Urban typology and building stock characteristics

Beijing and Shanghai, as highly urbanized megacities, have extensive building stocks that encompass a mix of residential and commercial structures, ranging from energy-intensive older buildings to newly constructed, energy-efficient ones (Pan et al., 2019). Shenzhen, a rapidly expanding technology hub, stands out for its modern urban development and strong emphasis on sustainability, with a growing number of green buildings shaping its cityscape (Güneralp & Seto, 2008; Ng, 2002). In contrast, Harbin represents a mid-sized city where extreme cold climates and lower urban density present unique energy challenges. Its building stock includes both historic, energy-intensive structures reliant on centralized heating systems and newer, well-insulated constructions designed to withstand harsh winters (C. Liu et al., 2023). This variation in urban form, density, and climate across the selected cities provides a comprehensive foundation for analysing carbon reduction strategies in both retrofit and new construction scenarios. By examining the interplay between older, high-energy-demand buildings and emerging energy-efficient developments, these cities offer valuable insights into the pathways for achieving zero-carbon urban transitions in different climatic and urban contexts across China.

2.1.3. Data availability

Data availability is another factor influencing the selection of case study locations. The data required for the case study analysis includes baseline building constructions, materials, schedules, etc., for energy performance simulations across different building ages and heights. The reference building data for the simulations are sourced from the DeST database, which contains building prototype files with the data required for simulations (An et al., 2023).

Additional data required for the project includes superblock data, which classifies groups of building blocks in China as superblocks. For this purpose, a GIS database from an early study is used (Long et al., 2019). Other data needed for the project include building age, footprint, and building height data.

Since age data for buildings in China is not publicly available, data on the age of development areas is assumed to have a uniform age distribution and is obtained for selected sample superblocks from the Chinese Academy for Building Research (CABR). Footprint data from the publicly available Open-StreetMap is used to determine the size of the buildings (Geofabrik, 2024). The building height data used in the project is derived from the World Settlement Footprint 3D, which combines a modified human settlements mask from Sentinel-1 and Sentinel-2 imagery (10 m resolution) with 12 m digital elevation data and TanDEM-X radar imagery (Esch et al., 2022).

2.2 Work package B - establishing a baseline for building archetypes

In this work package of the project, the baseline for the building archetypes was established. The building archetypes were determined based on a study conducted by (An et al., 2023). According to the study, buildings are classified into four archetypes: Terraced House, Low-rise, High-rise Tower, and High-rise Slab. A prototype from each archetype was developed in a study using software called DeST (An et al., 2023). The classification process of the buildings is presented in Table 1.

As shown in Table 1, the geometrical information and natural ventilation rates for each prototype are provided. These four prototype buildings were modelled according to the energy standards applicable during that period. Therefore, this previous study serves as a valuable reference for this project, enabling the creation of DeST-based prototypes that can be converted into EnergyPlus models and further be used as baseline models in the project.

Table 1: The geometrica	Linformation and	d natural ventilation	n rates for	building archetypes.
rabio il riio godinionioa	i ii ii o i i i i a i a i i	a matarar vomanano.		bananig archietypee.

	Construction area (m²)	Air condition- ing area (m²)	Number of floors	Shape coefficient	Average window wall ratio	Natural ventilation (ACH)
Terraced house	1044	930	1-3	0.48	0.27	0.5–5
Low-rise	1795	1703	4-6	0.36	0.26	0.5–5
High-rise slab	4040	3947	7-17	0.31	0.26	0.5–5
High-rise tower	10261	10261	17<	0.30	0.25	0.5–5

To translate the DeST models generated in this study, both the published paper and the DeST software were utilized. A Python script was written to extract all data from the related Microsoft Access database files of the DeST software and store them in a MongoDB database. This allows for repeated use of the data to generate new models in EnergyPlus. The process of creating the MongoDB database is presented in Figure 3.

As shown in the figure, data is organized for each city (Beijing, Harbin, Shanghai, and Shenzhen), archetype (Terraced House, Low-rise, High-rise Slab, and High-rise Tower), and building age (determining the energy standard in force at the time). The stored building properties include construction and material details for surfaces such as walls, floors, and roofs. Additionally, activity schedules, including occupancy, lighting, and appliance usage, are acquired from DeST models and the published article of An et al. (2023). DeST prototype models use district heating and split AC for cooling. At this stage of the project, it was decided to simplify the DeST model by using ideal loads instead of an HVAC system in EnergyPlus. Therefore, the models were simulated with ideal loads rather than a detailed HVAC model. The next sections outline the subsequent steps taken in the model development process.

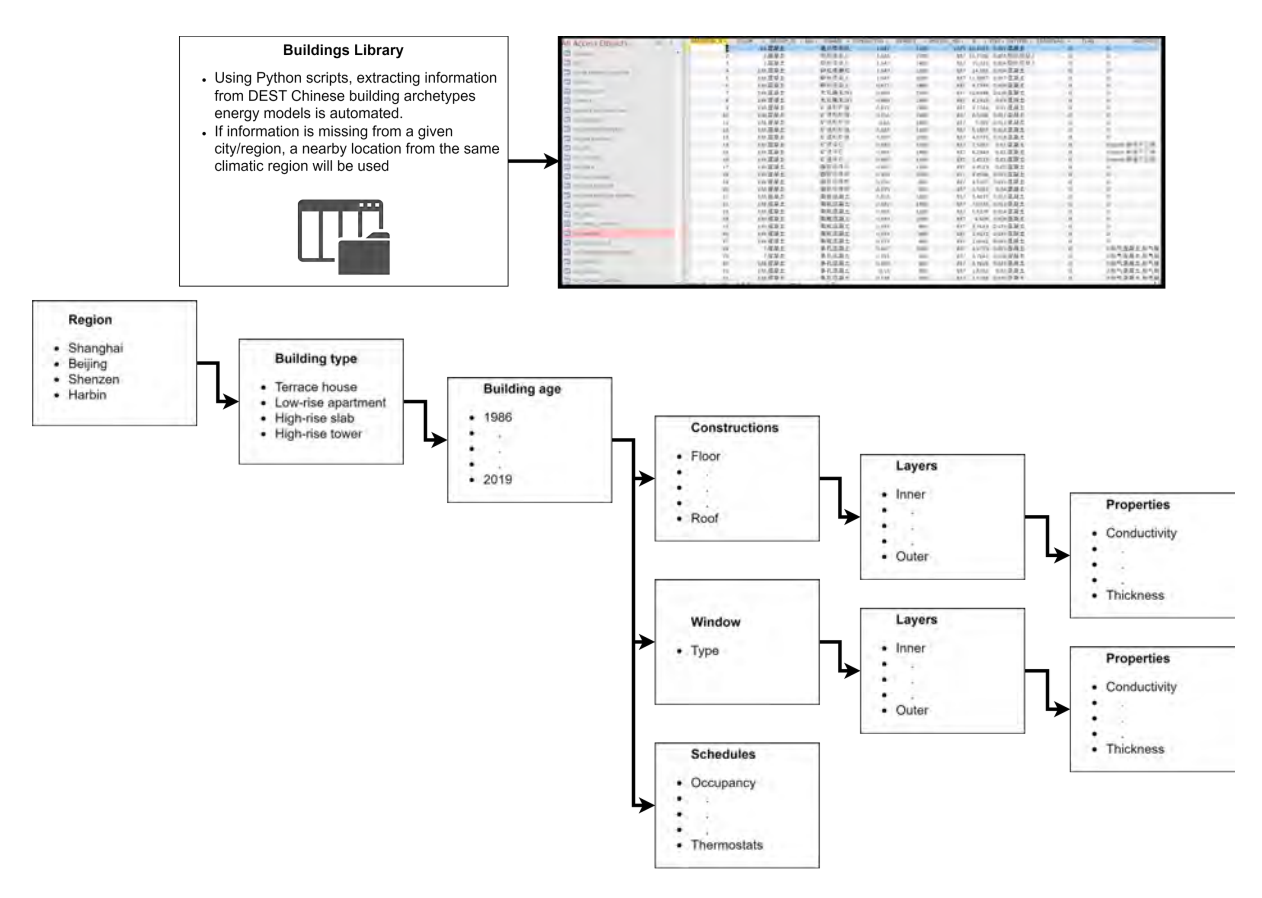


Figure 3: The process of translating and merging DeST database into MongoDB

2.2.1.Development of building models

The following elements were required to be generated individually because of the model differences and limitations.

- Modelling of the windows and glazing systems
- Schedules such as occupancy, usage of appliances and lighting etc.

The rest of the models were developed using the study by An et al. (2023) and DeST prototype building model files.

Window modelling:

The window modelling approach in DeST differs from that in EnergyPlus. Therefore, assumptions had to be made based on the information provided in the study on these prototype buildings. According to the database, all buildings use double glazing with ordinary glass and the same material type. However, when reviewing the article based on this database, it is evident that older buildings have significantly higher window U-values, likely due to the quality and age of the window frames. Unfortunately, the database does not provide detailed information about the frames, making it difficult to create a highly detailed EnergyPlus model.

For this reason, a simplified window model was chosen instead of a more detailed model based on multiple assumptions. The SIMPLEGLAZINGSYSTEM, which relies on three data points, U-factor, Solar Heat Gain Coefficient (SHGC), and Visible Transmittance, was implemented. These three values could be extracted from the database, and this approach is expected to produce results that align with those presented in the article.

Determining Schedules:

The prototype DeST models have schedules assigned to each room. However, our models use a simplified approach, treating each floor of the building as a single zone. Therefore, we needed to adapt our schedules to align with the detailed models presented in the article. The simplified schedules developed and presented in Figure 4 for this project can be considered a generalized version of those outlined in a previous study (An et al., 2023).

According to another reference, the average floor area of each apartment in China is 100 m², with one person occupying every 38.6 m² (H. Zheng et al., 2025). Therefore, if all occupants are at home, the models account for the heat load generated by people in the apartment, and the cooling of the buildings depends on the occupancy schedules. The occupancy schedule is also used for the cooling schedule. However, the model considers all values greater than 0 as 1, as it is not meaningful to partially cool a single zone. Consequently, we assume that the cooling loads in our EnergyPlus simulations will be higher compared to the results published in An et al. (2023) in the validation analysis.

The lighting and electric appliance schedules presented in the reference article are highly detailed, with separate schedules assigned to each room type. Given the simplified nature of our model, a representative schedule was developed to ensure compatibility while maintaining the overall energy profile. The derived schedules for lighting and appliances are presented below in Figure 4.

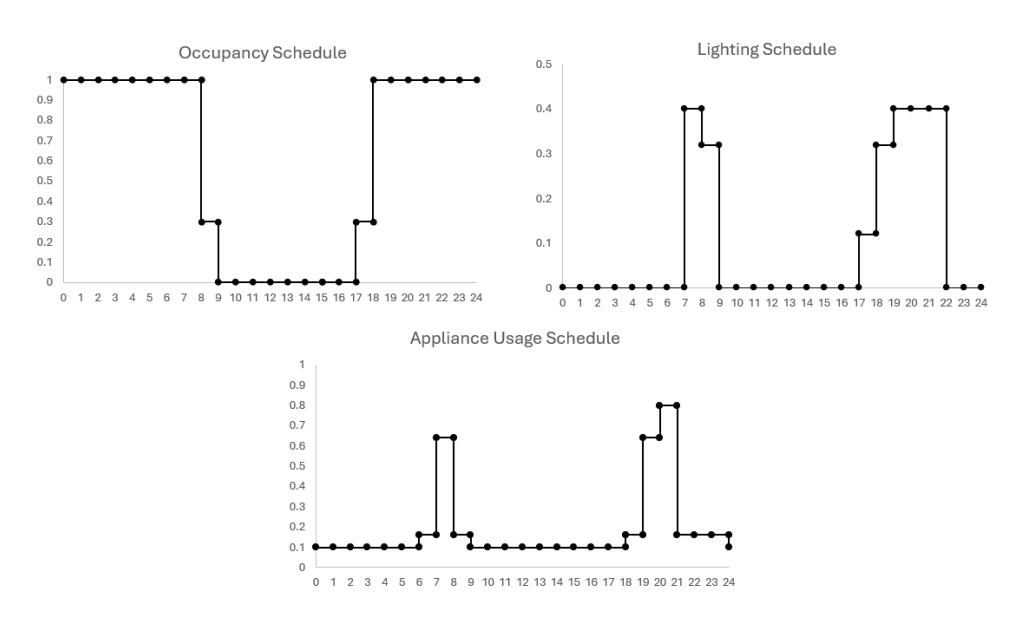


Figure 4: Schedules for Occupancy, Lighting, and Appliances

2.2.2.Results of the analysis

The baseline simulation results using EnergyPlus/Cesar-P were validated against the results for buildings constructed in Beijing between 2010 and 2018, as well as the findings from An et al. (2023), as shown in Figure 5. The baseline simulation results for buildings in Beijing constructed between 2010-2018 aligned with our anticipated differences but also showed that there is a general good agreement:

- DeST models incorporate complex geometries, particularly in terraced houses, while we used simplified geometries based on shape coefficients.
- Our simulations treat each floor as a single zone, whereas DeST simulations include detailed zones within each floor and apartment, with different schedules for each zone.
- Differences in window modelling between DeST and our transition to EnergyPlus required approximations.

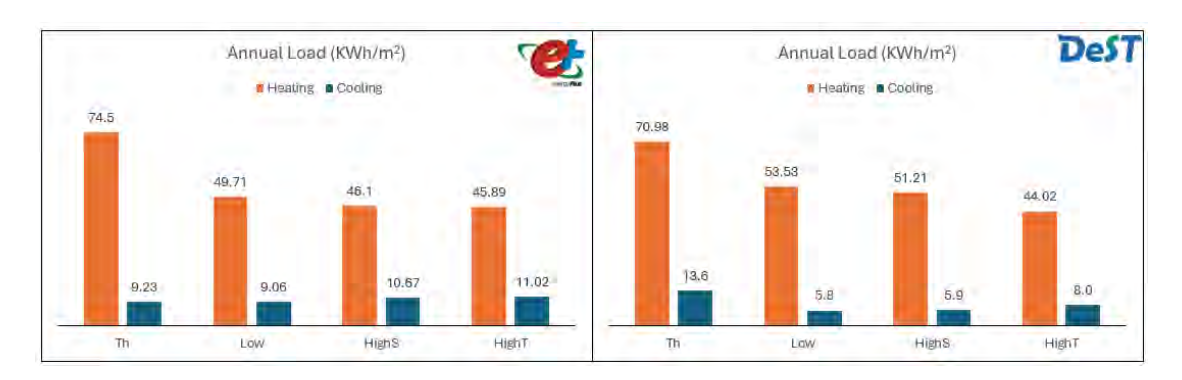


Figure 5: Comparison of EnergyPlus and DeST simulation results for Beijing 2010-2018.

Figure 6 presents the complete EnergyPlus simulation results for Beijing, Harbin, Shanghai, and Shenzhen. Beijing and Harbin are heating-dominated, while buildings in Shenzhen are more cooling-dominated. On the other hand, buildings in Shanghai have a more balanced heating and cooling load. As expected, after each standard update, the energy performance of the buildings generally improves. The results provide insights into the performance of each archetype in different climatic regions, and the models produced will serve as a foundation for the next stages of the project. Additionally, comparing the results with those in the reference paper confirms that the building models defined within EnergyPlus are well predicting the heating and cooling loads and can thus be used for further analysis.

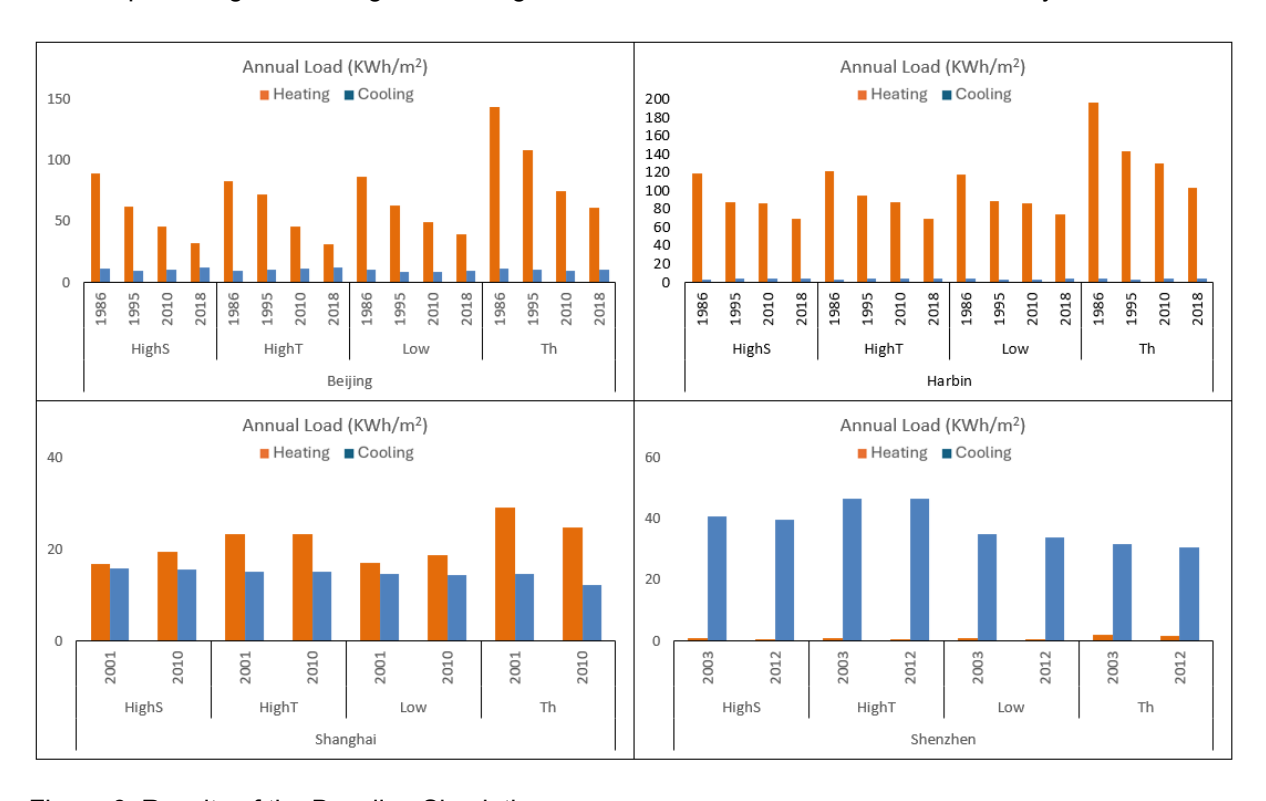


Figure 6: Results of the Baseline Simulations

2.3 Work package C - impact modelling of ZEB for archetype buildings

In the previous work package, building-level analysis was conducted to determine whether the models built in EnergyPlus using DeST produced results consistent with studies in the literature. In this work package, the building-level analysis continues, focusing on HVAC models and retrofit scenarios. The ZEB standard target values are used to identify the required modifications to the building properties (i.e.,

retrofits) to identify the necessary measures for achieving the required ZEB emissions. This includes fundamental improvements to the building envelope, building energy systems, and solar energy generation (rooftop PV). The differences between the baseline (without retrofit) and retrofitted building analysis results are used to quantify the impact of retrofits on each building archetype.

In this study, an improvement of building energy performance and an emission reduction is targeted by means of proposing tailored retrofit measures to existing buildings. It needs to be clarified that the results provided through this analysis equally hold for a replacement of an existing building by a new one featuring an equivalent energy and emission performance as the retrofitted one.

The steps taken in Work Package C are presented in Figure 7. As in the previous work package (B), all properties related to materials, constructions, geometry, and schedules are obtained from the DeST model database. For the HVAC systems (current/improved), sources from the literature are used to determine their characteristics. The retrofitting scenarios are defined and implemented based on values from the new ZEB standard, and the results are analysed to assess the impact of the ZEB standard at the building level.

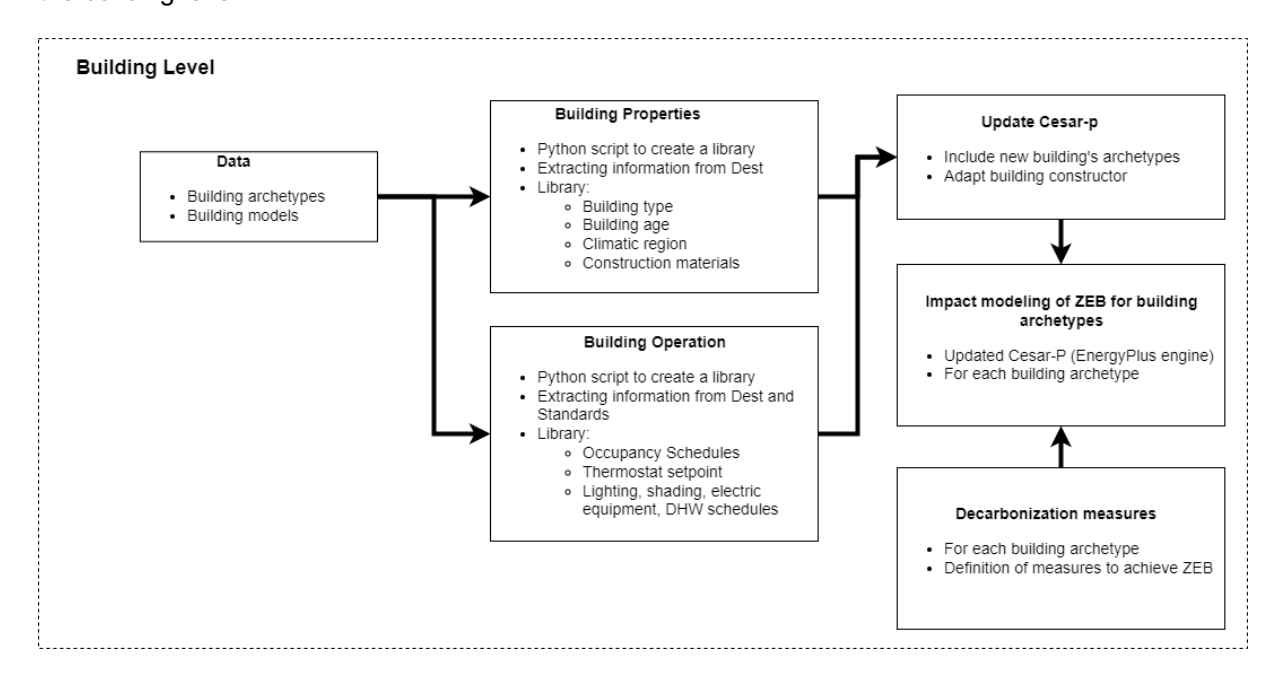


Figure 7: EnergyPlus/CESAR-P Archetype configuration – Building level

2.3.1. Determining current HVAC systems and possible improvements

In heating-dominated regions like Harbin and Beijing, most buildings use centralized gas heaters. They provide heat for both, the living spaces and the domestic hot water (DHW). On a larger scale, the district heating systems in North China, which serve multiple buildings or even whole neighbourhoods, mostly depend on coal or gas-powered plants that generate both electricity and heat (Su et al., 2018; L. Zhang et al., 2016). For retrofits, transitioning to centralized air-source heat pumps (ASHPs) provides a more energy-efficient alternative, aligning with China's ongoing efforts to phase out coal-based heating (Su et al., 2018). ASHPs have been promoted in rural areas as part of the coal-to-clean energy initiative and are increasingly used in urban settings. Space cooling remains unchanged, relying on decentralized split-unit air-air heat pumps, which are already common in these regions.

In cooling-dominated or more balanced climates (Shanghai and Shenzhen), decentralized split-unit airair heat pumps are widely used for both space heating and cooling due to their cost-effectiveness and adaptability in warm climates (Su et al., 2018). DHW in existing buildings is typically provided by decentralized gas heaters, which remain a practical choice given the availability of gas infrastructure in South China. The retrofit option replaces these with heat pump water heaters, which offer higher efficiency and

align with China's push toward electrification and improved building energy performance (G. Zheng & Bu, 2018).

Overall, these selections prioritize practical and scalable solutions, leveraging existing infrastructure while transitioning toward more energy-efficient and lower-emission alternatives. The selected HVAC system for the current and proposed state of the buildings is presented in Table 2.

Table 2: HVAC systems for the current and retrofitted design of the buildings

	Existing Building	Retrofit Option
	Heating Dominated Climate (H	arbin, Beijing)
Space Heating	Centralized gas heater	Centralized air-source hp
DHW	Centralized gas heater	Centralized air-source hp
Space Cooling	Decentralized split unit (air-air hp)	Decentralized split unit (air-air hp
	Cooling Dominated Climate (Sha	nghai. Shenzhen)
		J . , ,
Space Heating	Decentralized split unit (air-air hp)	Decentralized split unit (air-air hp)
Space Heating DHW	<u> </u>	•

2.3.2.Decarbonization pathways

The transition towards low-carbon buildings requires a strategic combination of passive and active measures to enhance energy efficiency and reduce carbon emissions. Table 3 outlines a series of decarbonization pathways designed to improve the energy performance of buildings. These measures progressively incorporate insulation upgrades, window replacements, HVAC system improvements, onsite renewable energy generation, and shading elements. A key aspect of decarbonization is reducing heat losses through the building envelope. Ground floor insulation, roof insulation, and wall insulation are systematically introduced across different pathways, minimizing heating and cooling demand. Windows are also upgraded in determined measures to further improve thermal performance and reduce energy losses.

The insulation thicknesses and window upgrades were made based on the GB/T 51350-2019 Near-Zero Energy Buildings Standard of China (MoHURD, 2019). This standard defines different U-values for building components depending on the climate region to optimize energy efficiency. For windows, the selected glazing has a U-value of 1.2 W/m²K in Beijing, 1.0 W/m²K in Harbin, 2.0 W/m²K in Shanghai, and 2.5 W/m²K in Shenzhen, all with a fixed solar heat gain coefficient (SHGC) of 0.30. Wall insulation was designed to achieve U-values of 0.20 W/m²K in Beijing, 0.15 W/m²K in Harbin, 0.40 W/m²K in Shanghai, and 0.80 W/m²K in Shenzhen, ensuring effective thermal performance for different heating and cooling needs. Roof insulation follows a similar climate-based approach, with U-values of 0.15 W/m²K in Beijing and Harbin, 0.25 W/m²K in Shanghai, and 0.35 W/m²K in Shenzhen. Lastly, for ground floors, a uniform U-value of 0.30 W/m²K is applied across all locations. These values ensure that insulation strategies are tailored to each city's climate, enhancing building energy efficiency and thermal comfort.

Decarbonization strategies include enhancements in HVAC efficiency and replacing conventional systems with more energy-efficient alternatives. These improvements contribute significantly to reducing operational emissions and optimizing energy use for heating, cooling, and domestic hot water. The proposed systems are presented in Table 2. Several pathways incorporate roof-top photovoltaic (PV) panels to generate renewable electricity on-site. The inclusion of PV panels in later pathways contributes to the transition towards net-zero energy buildings by offsetting grid electricity consumption with clean energy production. In addition to active system improvements, shading elements are introduced in some scenarios to enhance thermal comfort and reduce cooling loads. These passive measures help limit

solar heat gains, particularly in cooling-dominated climates, thereby reducing reliance on mechanical cooling systems.

The pathways presented in Table 3 follow a stepwise approach, gradually incorporating additional measures to optimize effort for retrofitting and performance. Basic insulation and window upgrades form the foundation, while more advanced strategies, such as HVAC upgrades, PV integration, and shading elements, are introduced progressively. The final pathway integrates all measures, representing the most comprehensive approach to decarbonization. By adopting these pathways, buildings can achieve significant reductions in energy demand and carbon emissions, contributing to broader climate and sustainability goals.

Table 3: Decarbonization pathways determined for energy performance improvement

#Measure	Ground Floor Insulation	Roof Insulation	Wall Insulation	Windows Upgrade	HVAC Improvement	PV Panels	Shading Elements
1	+	+		+			
2	+	+	+	+			
3	+	+		+	+		
4	+	+	+	+	+		
5	+	+		+	+	+	
6	+	+	+	+	+	+	
7	+	+		+			+
8	+	+	+	+			+
9	+	+		+	+		+
10	+	+	+	+	+		+
11	+	+		+	+	+	+
12	+	+	+	+	+	+	+

2.3.3. Carbon emission calculations

The new ZEB standard evaluates the performance of buildings based on the carbon emission intensity per square meter of floor area. In this project, the net operational carbon emissions are calculated and used as a benchmark to compare the performance of retrofitting measures. Therefore, embodied carbon emissions are not taken into consideration. The calculated carbon emissions are compared against the corresponding emission thresholds for residential buildings, as presented in Table 4 (MoHURD, 202X).

Table 4: Nearly zero carbon residential building carbon dioxide emission intensity (kgCO₂eq/m²y).

Solar Irradiance Rating	Extremely Cold Zone	Cold Zone	Hot Summer and Cold Winter Zone	Hot Summer and Warm Winter Zone	Temperate Zone
I	14	13	1	1	1
- II	15	14	1	16	12
III	16	16	16	17	13
IV	/	1	1	17	14

To quantify the impact of the new regulation, energy performance results obtained from the simulations need to be converted into net carbon emission values. To this purpose, we used the carbon emission intensity for electricity and natural gas, which are the main energy sources used in HVAC and DHW systems of the buildings. According to a current study, China's comprehensive electricity footprint is 0.6835 tCO₂eq/MWh (Q. Zhang et al., 2024). The carbon emission intensity of natural gas from well to gate, considering the 104 fields in China, ranges from 0.022 to 0.156.3 kgCO₂eq/kWh, with a weighted average carbon emission intensity of 0.078 kgCO₂eq/kWh (Gan et al., 2020). The carbon emission

intensity of the combustion of natural gas is 0.180–0.216 kgCO₂eq/kWh (Venkatesh et al., 2011). The value used for the calculation of natural gas carbon emission intensity is 0.276 kgCO₂eq/kWh.

2.3.4. The results of the analysis

The analysis results indicate that carbon emissions from electric appliances and lighting in the buildings amount to 18.23 kgCO₂eq/m²/year. Given that the electricity grid's carbon emission intensity of 0.6835 kgCO₂eq/kWh cannot be reduced, these buildings are unable to meet the nearly zero-carbon thresholds (Table 4) specified in the new zero-carbon building standard without the addition of PV panels. In Table 5 presents results specifically influenced by building retrofit interventions - focusing exclusively on HVAC and domestic hot water (DHW) system emissions. The complete results, including emissions from electrical appliances and lighting, are shown in Table 6.

Table 5: Simulation results of the building level analysis under defined measures, considering HVAC and DHW systems (kgCO₂eq/m²y).

10 -		0.4	20.0						17.4	0.2	100	200	D ***	TT' 1 C	0 100-
-10.6	-4.6	9.4	15.4	7.7	15,4	-9.2	-3.7	10.8	16.4	9.2	16.3	35.2	Beijing	HighS	0 1986
1.8	5.7	9.3	13.2	7.7	12.5	3.1	6.8	10.6	14.3	9.1	13.6	32.3	Beijing	HighT	1 1986
-34.7	-29.5	10.4	15.6	8.6	15.1	-33.7	-28.7	11.3	16.4	9.5	15.7	32.8	Beijing	Low	2 1986
-77.0	-69.2	13/1	20.9	11.9	21.4	-76.0	-68.0	14.1	22.1	12.7	22.7	55.8	Beijing	Th	3 1986
-10.7	-9.2	9.3	10.8	7.7	9.5	-9.3	-8.0	10.8	12.0	9.1	10.7	22.9	Beijing	HighS	4 1995
1.8	5.7	9.3	13.2	7.7	12.5	3.1	6.8	10.6	14.3	9.1	13.6	26.8	Beijing	HighT	5 1995
-34.8	-33.3	10.3	11.8	8.5	10.2	-33.8	-32.3	11.3	12.8	9.5	11.2	22.5	Beijing	Low	6 1995
-77.3	-74.9	12.9	15.2	11.6	14.6	-76.1	-73.8	13,9	16,3	12.5	15.6	38.0	Beijing	Th	7 1995
-10.7	-8.4	9.3	11.7	7.7	10.4	-9.3	-7.2	10.7	12.8	9.1	11.6	17.8	Beijing	HighS	8 2010
1.7	4.3	9.2	11.8	7.7	10.7	3.1	5.4	10.6	12.9	9.1	11.8	17.8	Beijing	HighT	9 2010
-34.8	-33.1	10.3	12.0	8.5	10.5	-33.8	-32.1	11.3	13.0	9.4	11.4	17.9	Beijing	Low	10 2010
-77.3	-75.5	12.8	14.6	11.6	13.7	-76.2	-74.4	13.9	15.7	12.4	14.7	25.0	Beijing	Th	11 2010
-10.7	-10.2	9.3	9.8	7.6	8.3	-9.3	-8.9	10.7	11.2	9.1	9.6	13.2	Beijing	HighS	12 2018
1.7	2.3	9.2	9.8	7.7	8.4	3.1	3.6	10.6	11.1	9.1	9.6	12.9	Beijing	HighT	13 2018
-34.8	-34.2	10.2	10.9	8.4	9.2	-33.8	-33.2	11.2	11.9	9.4	10.1	14.4	Beijing	Low	14 2018
-77.4	-76.3	12.8	13.8	11.6	12.9	-76.2	-75.3	13.8	14.8	12.4	13.7	20.2	Beijing	Th	15 2018
-4.5	1.6	11.7	17.8	9.9	17.9	-3.5	2.3	12.7	18.5	11.0	18.8	35.6	Harbin	HighS	16 1986
5,5	12.1	11.6	18.2	9.9	18.6	6.5	12.9	12.6	18.9	11.0	19.1	36,2	Harbin	HighT	17 1986
-23.3	-18.7	13.1	17.8	11.4	17.6	-22.5	-18.0	13.9	18.5	11.9	18.3	35.4	Harbin	Low	18 1986
-55.9	-46.9	16.9	25.9	15.8	27.5	-55.2	-46.1	17.6	26,8	16.6	28.5	61.0	Harbin	Th	19 1986
-4.5	-1.9	11.7	14.3	9.9	13.4	-3.5	-1.1	12.7	15,1	11.0	14.2	24.6	Harbin	HighS	20 1995
5.5	9.7	11.6	15.8	9.9	15.1	6.5	10.5	12.6	16.6	10.9	16.2	26.4	Harbin	HighT	21 1995
-23.2	-21.2	13.2	15.2	11.4	13.9	-22.5	-20.5	13.9	15,9	11.9	14.8	24.7	Harbin	Low	22 1995
-55.8	-51.7	17.0	21.1	15.4	20.9	-55.2	-51.4	17.6	21.5	16.6	20.8	41.8	Harbin	Th	23 1995
-4.5	-0.3	11.7	15.9	10.0	15.2	-3.5	0.5	12.7	16.7	11.0	15.9	24.4	Harbin	HighS	24 2010
5.5	10.0	11.6	16.1	10.0	15.6	6.5	10.8	12.6	16.9	10.9	16.3	24.6	Harbin	HighT	25 2010
-23.2	-20.8	13.2	15.6	11.4	14.2	-22.5	-20.1	13.9	16.4	11.9	14.8	23.3	Harbin	Low	26 2010
-55.8	-53.4	17.0	19.4	16.1	18.9	-55.2	-52.8	17.6	20.1	16.5	19.6	36.6	Harbin	Th	27 2010
-4.4	-2.4	11.8	13.8	10.0	12.7	-3.5	-1.5	12.7	14.6	11.1	13.4	18.8	Harbin	HighS	28 2018
5,6	7.8	11.6	13.8	10.0	12.7	6.6	8.6	12.6	14.7	11.0	13.6	18.7	Harbin	HighT	29 2018
-23.1	-21.5	13.3	14.9	11.2	13.6	-22.4	-20.9	14.0	15.6	12.3	14.2	20.1	Harbin	Low	30 2018
-55.5	-54.0	17.3	18.8	15.9	18.3	-55.0	-53.4	17.9	19.4	16.3	18.8	26.8	Harbin	Th	31 2018
-0.5	5.9	16.1	22.5	14.1	20.4	0.3	6.6	16.8	23.2	14.8	21.2	26.6	Shanghai	HighS	32 2001
10.3	17.3	16.5	23.5	14.5	21.4	11.0	18.0	17.3	24.2	15.3	22.1	31.1	Shanghai	HighT	33 2001
-21.1	-16.2	16.2	21.1	14.2	19.0	-20.4	-15.6	16.9	21,7	15.0	19.7	27.2	Shanghai	Low	34 2001
-53.9	-45.0	20.7	29,5	18.7	27.5	-53.0	-44.2	21.6	30.4	19.6	28.4	40.9	Shanghai	Th	35 2001
-0.5	5.9	16.1	22.5	14.1	20.4	0.3	6.6	16.8	23.2	14.8	21.2	28.7	Shanghai	HighS	36 2010
10.3	17.3	16.5	23.5	14.5	21.4	11.0	18.0	17.3	24.2	15.3	22.1	31.1	Shanghai	HighT	37 2010
-21.1	-16.2	16.2	21.1	14.2	19.0	-20.4	-15.6	16.9	21.7	15.0	19.7	28.6	Shanghai	Low	38 2010
-53.9	-49.1	20.6	25.5	18.6	23.5	-53.1	-48.3	21.5	26.4	19.5	24.4	36.1	Shanghai	Th	39 2010
-2.3	-2.0	15.9	15.2	15.0	15.3	-1.1	-0.9	17.1	17.3	16.2	16.5	21.7	Shenzhen	HighS	40 2003
9.2	9.5	16.1	16.3	15.2	15.4	10.4	10.6	17.2	17.4	16.3	16.5	23.4	Shenzhen	HighT	41 2003
-24.9	-24.7	15.9	16.2	15.1	15.4	-23.8	-23.6	17.0	17,2	16.3	16.4	20.6	Shenzhen	Low	42 2003
-63.6	-63.2	18.1	18.4	17.3	17.7	-62.4	-62.0	19.4	19.7	18.6	18.9	23.6	Shenzhen	Th	43 2003
-2.4	-2.1	15.8	16.0	14.9	15.2	-1.2	-1.0	17.0	17.2	16.1	16.4	20.9	Shenzhen	HighS	44 2012
9.2	9.4	16.0	16.2	15.1	15.3	10.3	10.5	17.1	17,3	16.2	16.4	22.9	Shenzhen	HighT	45 2012
-25.0	-24.8	15.9	16.1	15.1	15.3	-23.9	-23.7	17.0	17.1	16.2	16.3	19.8	Shenzhen	Low	46 2012
-63.7	-63.4	18.0	18.3	17.2	17.5	-62.5	-62.2	19.3	19.5	18.6	18.8	22.1	Shenzhen	Th	47 2012

In Table 5 and Table 6, blue cells represent buildings that meet the nearly zero-carbon emission thresholds defined by China's Zero-Carbon Building Standard, as shown in Table 4. Green cells indicate buildings that are close to the threshold and have low carbon emissions. Yellow cells represent buildings

with moderate carbon emissions, while red cells highlight buildings with high carbon emissions. The results presented in Table 5 are important for demonstrating the effectiveness of each retrofitting measure, while Table 6 shows whether each building achieves the nearly-zero or net-zero carbon emission targets.

Table 6: Simulation results of the building-level analysis under measures including emissions from electric appliances and lighting (kgCO₂eq/m²y).

Vear	A rchetyne	Location	Raseline	Measure 1	Measure 2	Measure 3	Measure 4	Measure 5	Measure 6	Measure 7	Measure 8	Measure 9	Measure 10	Measure 11	Measure 12
0 1986	HighS	Beijing	53.6	34.7	27.6	34.8	29.2	14.7	9.2	33.8	26.1	33.8	27.8	13.8	7.8
1 1986	HighT	Beijing	50.7	32.0	27.5	32.7	29.0	25.2	21.5	30.9	26.1	31.6	27.7	24.1	20.2
2 1986	Low	Beijing	51.2	34.1	27.9	34.8	29.7	-10.3	-15.3	33.5	27.0	34.0	28.8	-11.1	-16.3
3 1986	Th	Beijing	74.2	41.1	31.1	40.5	32.5	-49.6	-57.6	39.8	30.3	39.3	31.5	-50.8	-58.6
4 1995	HighS	Beijing	41.3	29.1	27.5	30.4	29.2	10.4	9.1	27.9	26.1	29.2	27.7	9.2	7.7
5 1995	HighT	Beijing	45.2	32.0	27.5	32.7	29.0	25.2	21.5	30.9	26.1	31.6	27.7	24.1	20.2
6 1995	Low	Beijing	40.9	29.6	27.9	31.2	29.7	-13.9	-15.4	28.6	26.9	30.2	28.7	-14.9	-16.4
7 1995	Th	Beijing	56.4	34.0	30.9	34.7	32.3	-55.4	-57.7	33.0	30.0	33.6	31.3	-56.5	-58.9
8 2010	HighS	Beijing	36.2	30.0	27.5	31.2	29.1	11.2	9.1	28.8	26.1	30.1	27.7	10.0	7.7
9 2010	HighT	Beijing	36.2	30.2	27.5	31.3	29.0	23.8	21.5	29.1	26.1	30.2	27.6	22.7	20.1
10 2010	Low	Beijing	36.3	29.8	27.8	31.4	29.7	-13.7	-15.4	28.9	26.9	30.4	28.7	-14.7	-16.4
11 2010	Th	Beijing	43.4	33.1	30.8	34.1	32.3	-56.0	-57.8	32.1	30.0	33.0	31.2	-57.1	-58.9
12 2018	HighS	Beijing	31.6	28.0	27.5	29.6	29.1	9.5	9.1	26.7	26.0	28.2	27.7	8.2	7.7
13 2018	HighT	Beijing	31.3	28.0	27.5	29.5	29.0	22.0	21.5	26.8	26.1	28.2	27.6	20.7	20.1
14 2018	Low	Beijing	32.8	28.5	27.8	30.3	29.6	-14.8	-15.4	27.6	26.8	29.3	28.6	-15.8	-16.4
15 2018	Th	Beijing	38.6	32.1	30.8	33.2	32.2	-56.9	-57.8	31.3	30.0	32.2	31.2	-57.9	-59.0
16 1986	HighS	Harbin	54.0	37.2	29.4	36.9	31.1	20.7	14.9	36.3	28.3	36.2	30.1	20.0	13.9
17 1986	HighT	Harbin	54.6	37.5	29.4	37.3	31.0	31.3	24.9	37.0	28.3	36.6	30.0	30.5	23.9
18 1986	Low	Harbin	53.8	36.7	30.3	36.9	32.3	0.4	-4.1	36.0	29.8	36.2	31.5	-0.3	-4.9
19 1986	Th	Harbin	79.4	46.9	35.0	45.2	36.0	-27.7	-36.8	45.9	34.2	44.3	35.3	-28.5	-37.5
20 1995	HighS	Harbin	43.0	32.6	29.4	33,5	31.1	17.3	14.9	31.8	28.3	32.7	30.1	16.5	13.9
21 1995	HighT	Harbin	44.8	34.6	29.3	35.0	31.0	28.9	24.9	33.5	28.3	34.2	30.0	28.1	23.9
22 1995	Low	Harbin	43.1	33.2	30,3	34.3	32.3	-2.1	-4.1	32.3	29.8	33.6	31.6	-2.8	-4.8
23 1995	Th	Harbin	60.2	39.2	35.0	39.9	36.0	-33.0	-36.8	39.3	33.8	39.5	35.4	-33.3	-37.4
24 2010	HighS	Harbin	42.8	34.3	29.4	35.1	31.1	18.9	14.9	33.6	28.4	34.3	30.1	18.1	13.9
25 2010	HighT	Harbin	43.0	34.7	29.3	35.3	31.0	29.2	24.9	34.0	28.4	34.5	30.0	28.4	23.9
26 2010	Low	Harbin	41.7	33.2	30,3	34.8	32.3	-1.7	-4.1	32.6	29.8	34.0	31.6	-2.4	-4.1
27 2010	Th	Harbin	55.0	38.0	34.9	38.5	36.0	-34.4	-36.8	37.3	34.5	37.8	35.4	-35.0	-37.4
28 2018	HighS	Harbin	37.2	31.8	29.5	33.0	31.1	16.9	14.9	31.1	28.4	32.2	30.2	16.0	14.0
29 2018	HighT	Harbin	37.1	32.0	29.4	33.1	31.0	27.0	25.0	31.1	28.4	32.2	30.0	26.2	24.0
30 2018	Low	Harbin	38.5	32.6	30.7	34.0	32.4	-2.5	-4.0	32.0	29.6	33.3	31.7	-3.1	-4.7
31 2018	Th	Harbin	45.2	37.2	34.7	37.8	36.3	-35.0	-36.6	36.7	34.3	37.2	35.7	-35.6	-37.1
32 2001	HighS	Shanghai	45.0	39.6	33.2	41.6	35.2	25.0	18.7	38.8	32.5	40.9	34.5	24.3	17.9
33 2001	HighT	Shanghai	49.5	40.5	33.7	42.6	35.7	36.4	29.4	39.8	32.9	41.9	34.9	35,7	28.7
34 2001	Low	Shanghai	45.6	38.1	33.4	40.1	35.3	2.8	-2.0	37.4	32.6	39.5	34.6	34.7	-2.7
35 2001	Th	Shanghai	59.3	46.8	38.0	48.8	40.0	-25.8	-34.6	45.9	37.1	47.9	39.1	-26.6	-35.5
36 2010	HighS	Shanghai	47.1	39,6	33,2	41.6	35,2	25.0	18.7	38.8	32,5	40.9	34,5	24.3	17.9
37 2010	HighT	Shanghai	49.5	40.5	33.7	42.6	35.7	36.4	29.4	39.8	32.9	41.9	34.9	35.7	28.7
38 2010	Low	Shanghai	47.0	38.1	33.4	40.1	35.3	2.8	-2.0	37.4	32.6	39.5	34.6	34.7	-2.7
39 2010	Th	Shanghai	54.5	42.8	37.9	44.8	39.9	-29.9	-34.7	41.9	37.0	43.9	39.0	-30.7	-35.5
40 2003	HighS	Shenzhen	40.1	34.9	34.6	35.7	35.5	17.5	17.3	33.7	33.4	34.6	34.3	16.4	16.1
41 2003	HighT	Shenzhen	41.8	34.9	34.7	35.8	35.6	29.0	28.8	33.8	33.6	34.7	34.5	27.9	27.6
42 2003	Low	Shenzhen	39.0	34.8	34.7	35.6	35.4	-5.2	-5.4	33.8	33.5	34.6	34.3	-6.3	-6.5
43 2003	Th	Shenzhen	42.0	37.3	37.0	38.1	37.8	-43.6	-44.0	36.1	35.7	36.8	36.5	-44.8	-45.2
44 2012	HighS	Shenzhen	39.3	34.8	34.5	35.6	35.4	17.4	17.2	33.6	33.3	34.4	34.2	16.3	16.0
45 2012	HighT	Shenzhen	41.3	34.8	34.6	35.7	35.5	28.9	28.7	33.7	33.5	34.6	34.4	27.8	27.6
46 2012	Low	Shenzhen	38.2	34.7	34.6	35.5	35.4	-5.3	-5.5	33.7	33.5	34.5	34.3	-6.4	-6.6
47 2012	Th	Shenzhen	40.5	37.2	37.0	37.9	37.7	-43.8	-44.1	35.9	35.6	36.7	36.4	-45.0	-45.3

According to the results presented in Table 6, none of the baseline buildings meet the performance levels set by China's Zero-Carbon Building Standard. Among the archetypes, terraced houses perform the worst, exhibiting the highest baseline carbon emissions. In contrast, simulations under Measures 5, 6, 11, and 12 (which include the integration of PV panels) show that low-rise apartment buildings and terraced houses can generally achieve net-zero carbon emissions, thanks to a favourable ratio of PV panel area to total floor area. High-rise slab and tower buildings, however, typically fall short of even the nearly zero-carbon emission threshold.

To fully achieve net-zero carbon emissions, remaining emissions—particularly those not reducible at the building level—must be offset. Additionally, decarbonizing the electricity grid is essential to minimize the carbon intensity of energy consumption and ensure long-term alignment with net-zero goals.

2.4 Work package D - superblock analysis

As demonstrated in Figure 8, the superblock analysis consists of four main steps: data collection, data processing, baseline study, and scenario analysis. The objective of this work package is to cluster all available superblocks and identify representative archetypical ones. Once the representative superblocks are determined, they are simulated under various scenarios, including the baseline. The results are then used in the next work package for upscaling.

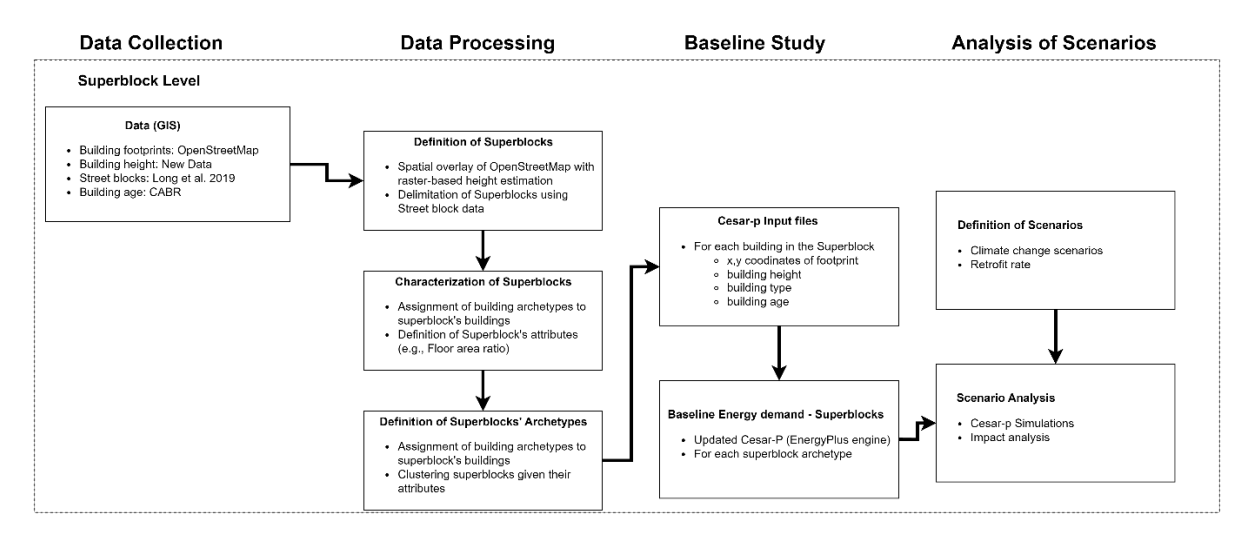


Figure 8: General framework for superblock level analysis

2.4.1. Data collection and processing

In the data collection and processing phases, the goal was to gather the necessary data for each city and apply k-means clustering to categorize superblocks into clusters, identifying a representative superblock for these clusters. As noted in the data availability section of Work Package A, the essential data for superblock-level analysis include building age, footprint, height, and superblock segmentation. The completeness of these datasets is crucial for conducting a reliable analysis at the superblock level. While minor data gaps can be addressed through manual completion, interpolation, or other analytical methods, a substantial lack of data prevents a comprehensive analysis across all superblocks and cities.

For this project, building height data, which is publicly available, was the only complete dataset. In contrast, building age data was entirely missing, and there were numerous gaps in building footprint data. Additionally, not all neighbourhoods were segmented into superblocks in the available dataset. The absence of building age data was the most significant limitation, as it was neither publicly available nor accessible from other sources. Ultimately, age data was provided by CABR for a limited number of buildings, as manually collecting data for a larger set of development areas would be unfeasible. Given these constraints, a selective methodology was the only feasible approach to conducting the analysis. The selected methodology is presented in Figure 9.

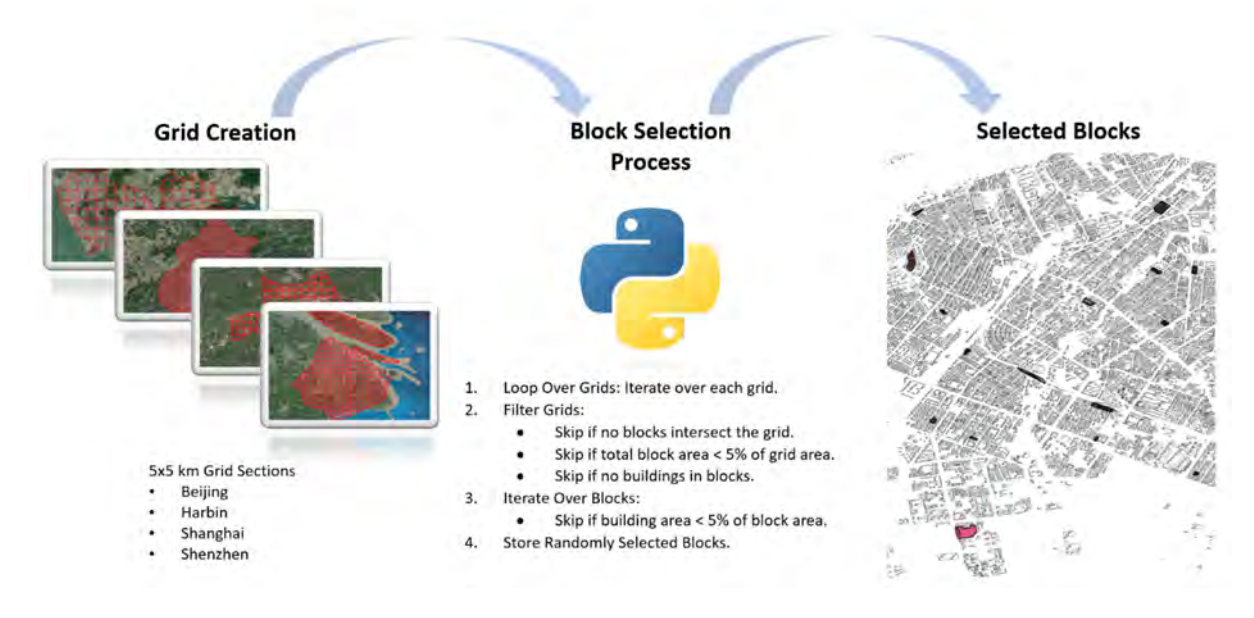


Figure 9: Superblock selection process

The building footprint and superblock datasets were merged for each city and divided into 5 km × 5 km grids. A semi-random selection process was applied using a Python script based on specific conditions: grid cells were skipped if no superblock data was available, if the total block area was smaller than 5% of the grid area, or if there was no building footprint data in the superblocks. Additionally, superblocks were excluded if the total building footprint area was smaller than 5% of the superblock area, as this indicated a high probability of missing building footprint data. The selected superblocks were recorded, and their information was stored in shapefiles for further analysis in the clustering process.

After the selection process, the data of the selected superblocks were reviewed, and it was observed that some building footprints were still missing. Since the number of missing data is limited due to the selective approach, these data were completed manually. Two example superblocks with missing building footprints are presented in Figure 10.

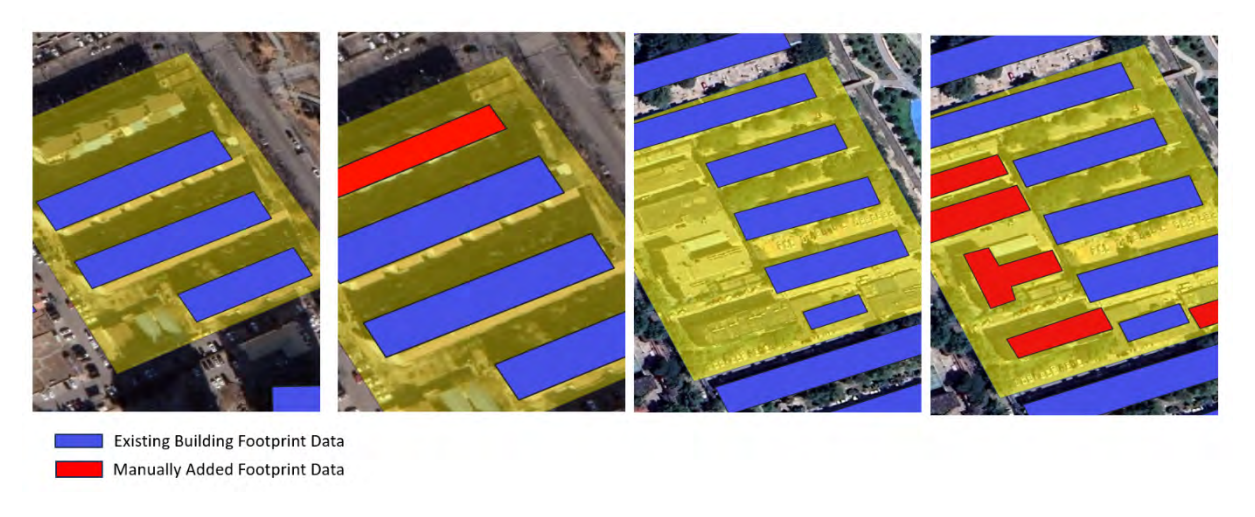


Figure 10: Completing missing data for building footprints

The data presented in Figure 11 demonstrates the distribution and density of selected superblocks across four cities: Beijing, Harbin, Shanghai, and Shenzhen. The top-left bar chart shows the number of sampled superblocks per city, indicating that Beijing has the highest number of samples (107), followed by Shanghai (58), Shenzhen (42), and Harbin (35). The top-right box plot presents the density distribution of superblocks, showing variations in density across cities. Superblock density is calculated by dividing the total floor area of the buildings (summing up across all storeys) on a superblock by the area of the superblock. Harbin and Shanghai present wider interquartile ranges and several outliers, suggesting more diverse spatial configurations. Superblocks in Beijing have the lowest density (1.44), while those in Shenzhen have the highest density (2.58).

The bottom stacked bar chart further details the distribution of different residential building archetypes within each city. While Beijing and Harbin have a significant proportion of low-rise apartments (45.8% and 40.9%, respectively), terrace houses dominate in Shanghai (58.6%) and Harbin (51.2%). High-rise slab buildings are more common in Shenzhen (37.6%) and Beijing (30.5%). In contrast, high-rise towers in the residential sector make up only a minor fraction across all cities, with negligible representation in Shenzhen and Harbin. The number of high-rise tower buildings is very low compared to other archetypes; only about 1.2% of the buildings in Beijing and Shanghai can be classified as high-rise towers.

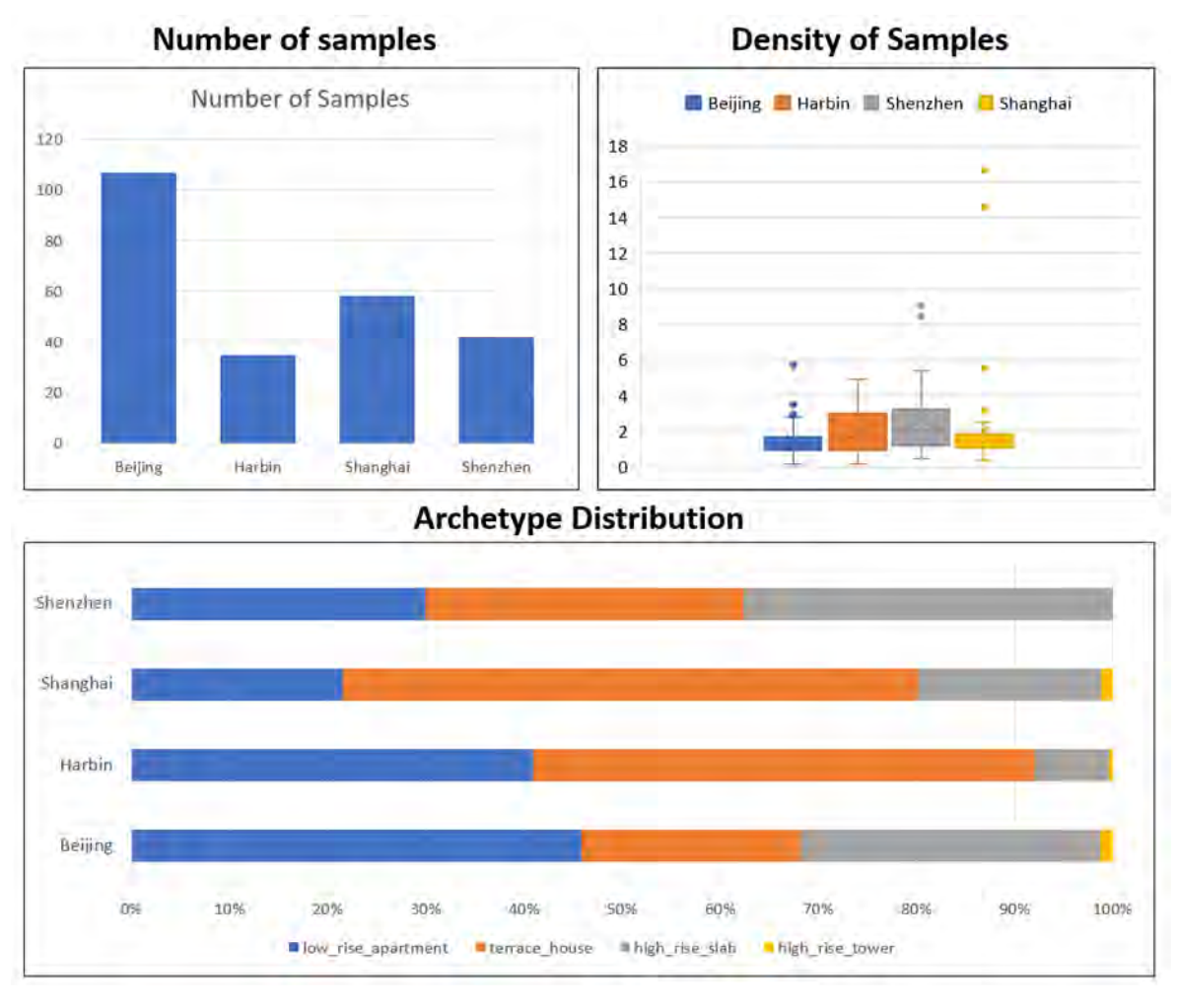


Figure 11: Simple statistics of selected superblocks

To further analyse the spatial characteristics of superblocks and determine the representative superblocks, the k-means clustering method was implemented to classify the superblocks based on their morphological and density-related attributes. k-means clustering is widely used due to its simplicity and

computational efficiency (Ikotun et al., 2023). This centroid-based method progressively refines the clusters through iterations until they converge to a final clustering outcome.

The selection of clustering parameters was guided by key urban form and density metrics that influence the spatial configuration of superblocks. The factors we used to cluster the superblocks are as follows: the average height of buildings within superblocks, the density of the superblocks, the age of the buildings, the shape factor of the buildings, the height-to-distance ratio of the buildings, and the average U-factor of the buildings. After a trial-and-error process, it was found that the results were most influenced by the density, shape factor, and U-factor parameters.

The density of the block is calculated by the total enclosed area/street block area:

$$Density = \frac{\sum_{1}^{n} FootPrint\ Area*Number\ of\ Floors}{Street\ Block\ Area}$$

The compactness of the buildings is calculated using the shape factor, which is simply the ratio between the volume of the building and the surface area of the building:

$$ShapeFactor_{Overall} = \frac{\sum_{1}^{n} Surface \ area \ of \ the \ building}{\sum_{1}^{n} Volume \ of \ the \ building}$$

The age data for buildings cannot be used directly because the building archetypes in the DeST data-base are categorized based on time intervals, making the age data categorical. Material properties of buildings change over time. For example, in the case of Beijing, there are four age categories: 1986, 1995, 2010, and 2018. Therefore, the age data is grouped into these categories. However, the k-means method does not work directly with categorical data. To apply k-means clustering, categorical data must be converted into numerical form, typically through one-hot encoding to create dummy binary variables. However, k-means is highly sensitive to categorical variables, and if a categorical parameter is included, the clustering results may be disproportionately influenced by these categories. To avoid this issue, the U-factor that closely correlates with building age (older buildings tend to have higher U-factors) was preferred as a clustering parameter instead of using age data. The overall U-factor for the superblocks are calculated using the following formula:

$$U-factor_{Overall} = \frac{\sum_{1}^{n} U - factor_{i} \times SurfaceArea_{i}}{\sum_{1}^{n} SurfaceArea_{i}}$$

The results of the clustering process are presented in Figure 12. Due to the larger volume of data available for Beijing, the clustering results for this city are more refined, with each cluster appearing more distinct compared to the other cities. Specifically, Beijing has 4 clusters, Harbin has 3, and Shanghai and Shenzhen have 2 clusters each. The determination of the optimal number of clusters was based on a trial-and-error process to ensure the most meaningful grouping of data points.

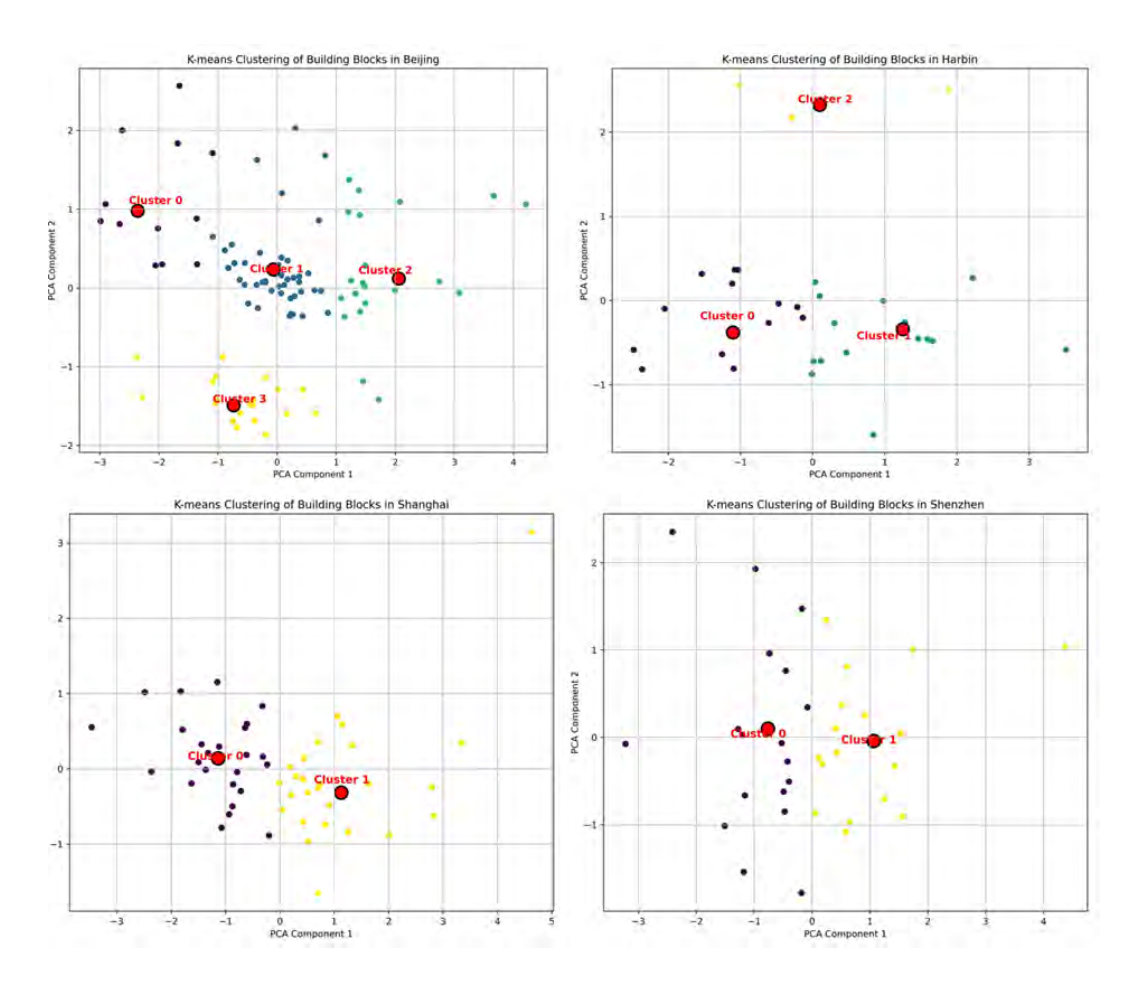


Figure 12: Clustering analysis with principal component visualization

The exploratory statistical analysis was conducted after determining the clusters and representative superblocks, with results presented in Figure 13.

Beijing dataset consists of 107 samples divided into 4 clusters. Cluster 0 represents highly dense blocks with a low shape factor and a moderate U-factor. Cluster 1 has moderate density, shape factor, and U-factor. Cluster 2 has the lowest density, a high shape factor, and the lowest U-factor. Cluster 3 consists of moderately dense blocks with a moderate shape factor but the highest U-factor, indicating lower thermal performance.

Harbin dataset consists of 35 samples and is grouped into 3 clusters, Cluster 0 represents high-density blocks with a lower shape factor and a moderate U-factor. Cluster 1 has the lowest density, a moderate shape factor, and the lowest U-factor. Cluster 2 has average density, a high shape-factor value, and the highest U-factor, suggesting lower thermal performance.

The Shanghai dataset contains 58 samples divided into two clusters. Cluster 1 represents high-density blocks with lower shape-factor values and slightly higher U-factor values than Cluster 0, which has a lower density, higher shape-factor value, and lower U-factor value.

Shenzhen comprises 36 samples and has two clusters. Cluster 1 consists of high-density blocks with regular shapes and slightly higher U-factors, while Cluster 0 includes less dense blocks with irregular shapes and moderate U-factors.

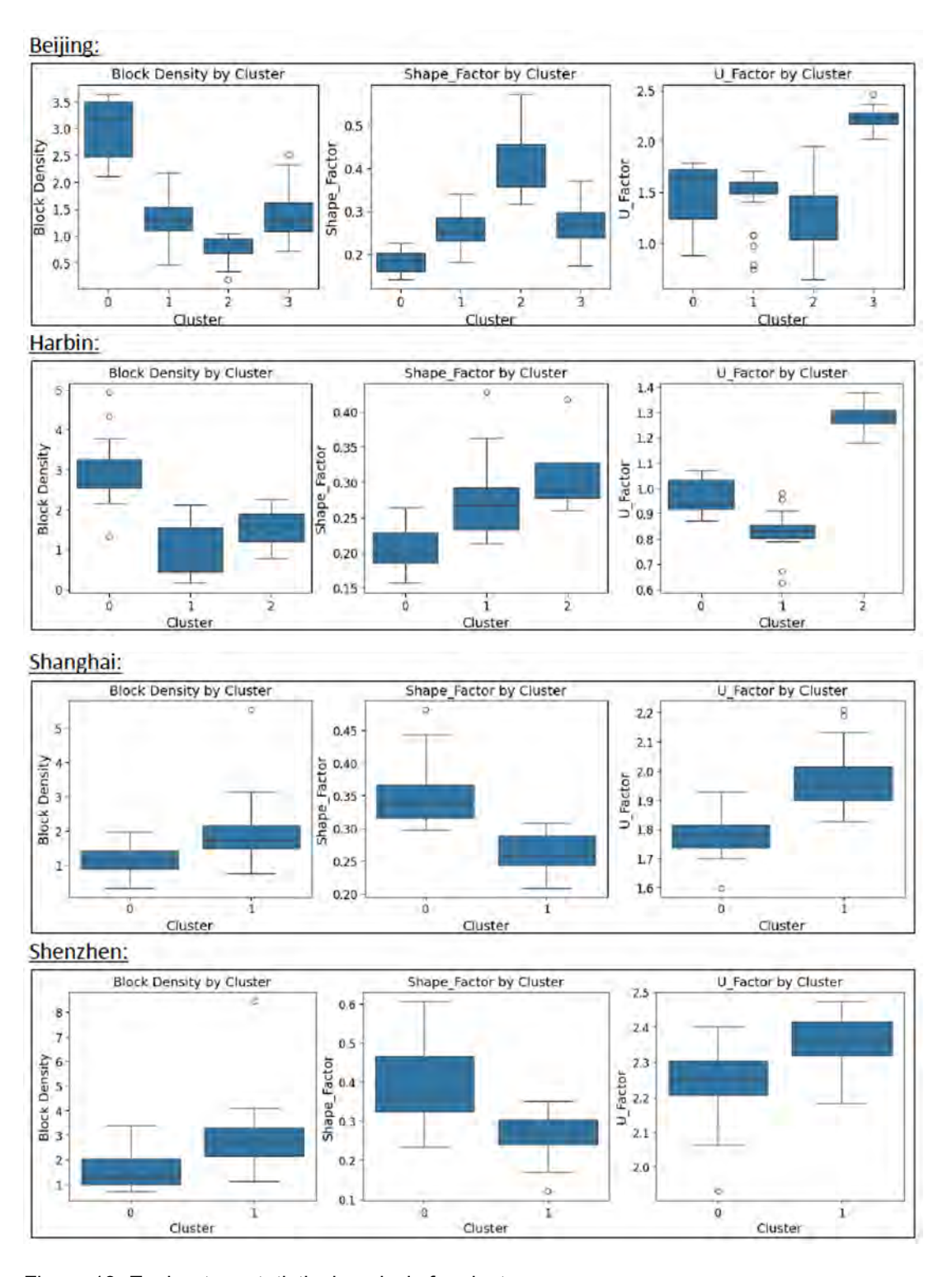


Figure 13: Exploratory statistical analysis for clusters

Generally, high-density clusters across all datasets typically have lower shape-factors and moderate to high U-factors. In contrast, low-density clusters (e.g., Cluster 2 in Beijing) tend to have moderate to high shape factors and lower U-factors.

Despite data limitations, the k-means clustering process identified meaningful patterns in density, shape factor, and U-factor, demonstrating its effectiveness in capturing distinct morphological and thermal properties.

Beijing – Representative Superblocks

Figure 14 presents the selected superblocks, representing clustered superblocks in Beijing. General information about each representative block is discussed below:

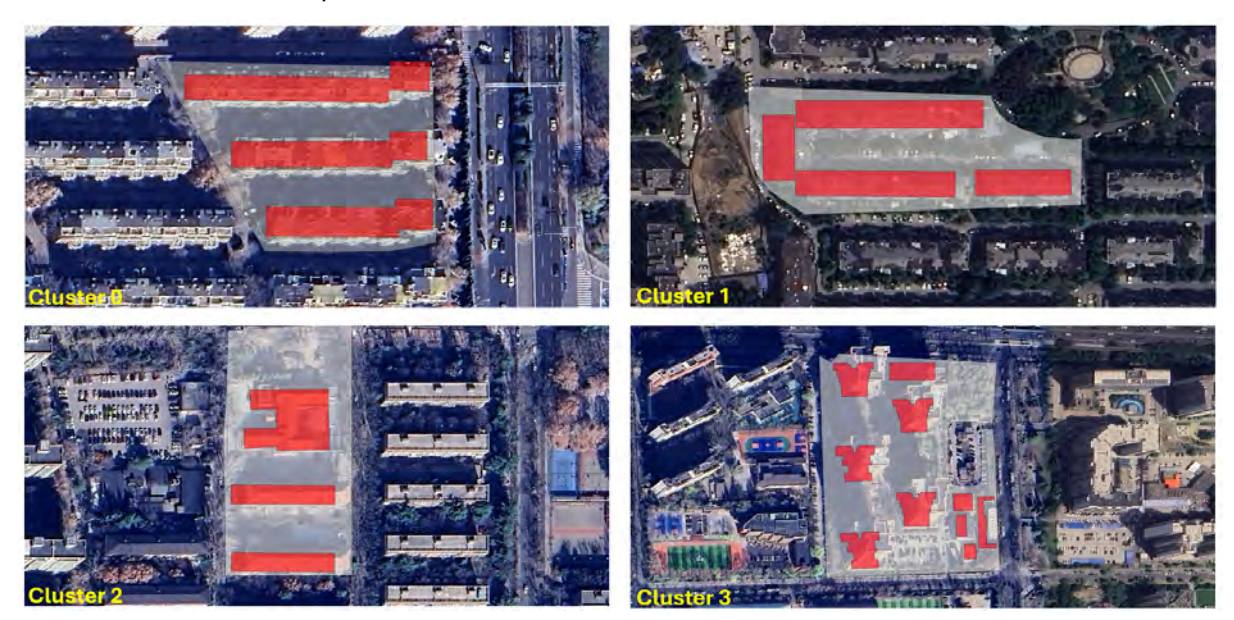


Figure 14: Representative clusters for Beijing

Beijing Cluster 0:

The representative superblock of Cluster 0 in Beijing exhibits a block density of approximately 3.63, indicating a densely built-up area. The median building height is 35.9 meters. The block contains three buildings spread across a block area of about 7523 square meters, with a shape factor of 0.265, which may reflect buildings with compact layouts. The construction date of the buildings in this block is classified based on U-factors as 1995 according to DeST database archetypes. The overall U-factor of the representative superblock is 1.70 W/m²K, indicating a moderate thermal performance compared to other representative superblocks in Beijing.

Beijing Cluster 1:

The representative superblock of Cluster 1 in Beijing has a block density of approximately 1.53, indicating a less dense built environment than Cluster 0. The median building height is 11.55 meters suggesting relatively low-rise buildings. The block contains four buildings spread across an area of approximately 9,728 square meters, with a shape factor of 0.332, indicating a moderately compact layout. Based on the age data the buildings in this block were built between 1995 and 2010, thus, according to the DeST database 1995 is considered the construction date for modelling purposes. The overall U-factor of the representative superblock is 1.52 W/m²K, reflecting a relatively good thermal performance compared to other representative superblocks in Beijing.

Beijing Cluster 2:

The representative superblock of Cluster 2 in Beijing has a block density of approximately 0.61, indicating a relatively low-density built environment. The median building height is 7 meters, suggesting predominantly low-rise buildings. The block contains three buildings spread across an area of approximately 12,029 square meters, with a shape factor of 0.439, reflecting a

comparatively dispersed layout. According to the DeST database archetypes, the buildings in this block are classified as having been built between 1995 and 2010, with 1995 considered as the construction date for modeling purposes. The overall U-factor of the best-performing representative superblock is 1.35 W/m²K, indicating the highest thermal performance among the representative superblocks in Beijing.

Beijing Cluster 3:

The representative superblock of Cluster 3 in Beijing has a block density of approximately 1.27, indicating a moderately dense built environment. The median building height is 18.3 meters, with a height-to-distance ratio of 1.22, suggesting mid-rise buildings with a balanced spacing. The block contains ten buildings spread across an area of approximately 37,481 square meters, with a shape factor of 0.279, reflecting a relatively open layout. According to the DeST database archetypes, the buildings in this block are classified as having been built between 1986 and 1995, with 1986 considered as the construction date for modeling purposes. The overall U-factor of the representative superblock is 2.34 W/m²K, which indicates the lowest thermal performance compared to other representative superblocks in Beijing.

Harbin – Representative Superblocks

Figure 15 presents the selected superblocks, representing clustered superblocks in Harbin. General information about each representative block is discussed below:



Figure 15: Representative clusters for Harbin

Harbin Cluster 0:

The representative superblock in Harbin has a block density of approximately 3.18, indicating a densely built-up area. The median building height is 26.3 meters, with a height-to-distance ratio of 3.76, suggesting mid to high-rise buildings positioned relatively close to each other. The block contains six buildings spread across an area of approximately 15,496 square meters, with a shape factor of 0.278, reflecting a compact layout. According to the DeST database archetypes, the buildings in this block are classified as having been built in 2010. The weighted average U-

factor of the superblock is 0.98 W/m²K, indicating its thermal performance is moderate compared to other representative superblocks.

Harbin Cluster 1:

The representative superblock of this cluster in Harbin has a block density of approximately 0.96, indicating a moderately dense built environment. The median building height is 13.6 meters. The block contains 14 buildings spread across an area of approximately 35,721 square meters, with a shape factor of 0.357, reflecting moderately compact structures. According to the DeST database archetypes, the buildings in this block are classified as having been constructed between 1995 and 2010, with 1995 used as the construction date for modeling purposes. The overall U-factor of the superblock is 0.89 W/m²K, reflecting the building's envelope performance as the best among the representative superblocks in Harbin.

Harbin Cluster 2:

The representative superblock of this cluster has a block density of approximately 1.35, indicating a relatively dense built environment. The median building height is 12.6 meters. The block consists of 7 buildings covering an area of approximately 14,166 square meters, with a shape factor of 0.368, reflecting moderately compact structures. Based on the DeST database archetypes, the buildings in this block are classified as having been constructed around 1986, which is used as the construction date for modeling purposes. The weighted average U-factor of the superblock is 1.37 W/m²K, indicating its thermal performance to be the lowest.

Shanghai – Representative Superblocks

Figure 1Figure 16 presents the selected superblocks, representing clustered superblocks in Shanghai. General information about each representative block is discussed below:





Figure 16: Representative clusters for Shanghai

Shanghai Cluster 0:

The representative superblock of this cluster has a block density of approximately 1.12, indicating a moderately dense built environment. The median building height is 10.4 meters, with 19 buildings distributed across an area of roughly 29,548 square meters. The shape factor of 0.411 reflects moderately compact structures. According to the DeST database archetypes, the buildings in this block are classified as having been constructed around 2001, which is used as the construction date for modeling purposes. The weighted average U-factor of the superblock is 1.88 W/m²K, indicating the envelope performance of the buildings.

Shanghai Cluster 1:

The representative superblock of this cluster has a block density of approximately 1.81, indicating a relatively high-density built environment. The median building height is 19.8 meters, with 18 buildings spread across an area of approximately 64,524 square meters. The shape factor of 0.249 suggests less compact, more elongated structures. Based on the DeST database

archetypes, the buildings in this block are classified as having been constructed around 2001, which is used as the construction date for modelling purposes. The weighted average U-factor of the superblock is 2.13 W/m²K, reflecting that the superblock's thermal insulation level is lower than that of the representative superblock for Cluster 0.

<u>Shenzhen – Representative Superblocks</u>

Figure 17 presents the selected superblocks, representing clustered superblocks in Shenzhen. General information about each representative block is discussed below:





Figure 17: Representative clusters for Shenzhen

Shenzhen Cluster 0:

The representative superblock of this cluster has a block density of approximately 1.40, indicating a moderately dense built environment. The median building height is 13 meters, with 29 buildings distributed across an area of roughly 56,381 square meters. The shape factor of 0.359 reflects moderately compact structures. According to the DeST database archetypes, the buildings in this block are classified as having been constructed around 2003, which is used as the construction date for modelling purposes. The weighted average U-factor of the superblock is 2.25 W/m²K, indicating its insulation level.

Shenzhen Cluster 1:

The representative superblock of this cluster has a block density of approximately 3.26, indicating a highly dense built environment. The median building height is 24.3 meters, with 45 buildings spread across roughly 76,719 square meters. The shape factor of 0.267 suggests less compact, more elongated structures. Based on the DeST database archetypes, the buildings in this block are classified as having been constructed around 2003, which is used as the construction date for modelling purposes. The weighted average U-factor of the superblock is 2.35 W/m²K, reflecting its thermal performance.

2.4.2. Baseline and scenario analysis

At this stage of the project, the selected clusters are simulated to calculate their energy demand under baseline and various scenario conditions. The baseline properties of the buildings are determined using data from the DeST database, while the scenario conditions are guided by the results from the building-level analysis. Representative superblocks are simulated for the baseline and six scenario conditions to assess their energy performance and decarbonization potential. The scenarios are summarized in Table 7.

The scenarios are defined as follows: The Baseline (Scenario 0) represents the current building conditions. Scenario 1 incorporates 100% improved insulation and controlled shading (passive measures), while Scenario 2 focuses on the full adoption of air-source heat pumps combined with photovoltaic (PV) systems (active measures). Scenario 3 combines all measures from Scenarios 1 and 2, integrating both passive and active strategies. Scenarios 4 to 7 extend Scenarios 0 to 3 by incorporating projected climate change impacts under the SSP2-4.5 scenario (a moderate emissions pathway where global 32/51

temperatures rise ~2.7°C by 2100). This was achieved by generating future weather files from current reference weather data to reflect the anticipated climatic conditions. These scenarios adjust future temperature, humidity, and extreme weather projections to assess the building's long-term resilience under changing climatic conditions. Additionally, the scenarios were evaluated under varying electricity carbon intensities (25%, 50% and 90%) to assess the impact of grid decarbonization.

Table 7: Decarbonization Pathways Determined for Energy Performance Improvement

#Scenario	Ground Floor Ins.	Roof Ins.	Wall Ins.	Windows Upgrade	HVAC Improvement	PV Panels	Shading Elements	Global Warming
Baseline	-	-	-	-	-	-	-	-
Scenario 1	+	+	+	+	-	-	+	-
Scenario 2	-	-	-	-	+	+	-	-
Scenario 3	+	+	+	+	+	+	+	-
Scenario 4	-	-	-	-	-	-	-	+
Scenario 5	+	+	+	+	-	-	+	+
Scenario 6	-	-	-	-	+	+	-	+
Scenario 7	+	+	+	+	+	+	+	+

The decarbonization analysis is extended from the building level to the superblock, and district level, focusing on archetype superblocks. The results from the superblock simulations are used to identify which scenarios have the greatest impact on energy demand and carbon emissions across the various superblocks. The simulation results excluding carbon emissions from electric appliances and lighting are presented in Table 8.

Table 8: Results of the representative superblock analysis under defined scenarios, excluding electric appliances and lighting (kg CO₂eq/m²·y).

Cluste	r Location	Baseline	Scenario 1	Scenario 2	Scenario 3	Scenario 4	Scenario 5	Scenario 6	Scenario 7
0	Beijing	29.6	8.8	2.2	-8.7	28.2	10.4	3.2	-7.0
1	Beijing	28.0	8.4	-21.4	-31.8	26.8	9.8	-20.8	-30.3
2	Beijing	33.4	10.4	-69.2	-80.8	31.8	11.6	-69.2	-79.7
3	Beijing	23.9	9.3	-7.5	-15.3	23.5	10.6	-6.4	-13.9
0	Harbin	25.2	12.8	3.0	-3.5	23.1	12.7	2,4	-3.6
1	Harbin	29.4	12.1	-12.6	-21.6	26.4	11.9	-14.0	-21.9
2	Harbin	26.6	12.6	-11.3	-18.6	24,5	12.5	-12.2	-18.7
0	Shanghai	23.1	14.6	-9.6	-18.2	22.1	16.1	-12.3	-18.6
1	Shanghai	17.3	11.6	-0.3	-6.2	17.7	13.5	-1.3	-5.8
0	Shenzhen	18.4	15.0	-16.1	-19.5	24,0	19.6	-12.2	-16.7
1	Shenzhen	18.0	14.4	0.8	-2.8	23,3	18.3	5.2	0.2

As can be seen in Table 8, all scenarios result in reduced emissions compared to the Baseline. Scenarios 3 and 7, which include the most comprehensive energy efficiency measures, consistently show the lowest emissions, reflecting the most effective decarbonization strategies. HVAC improvements, especially when combined with PV panels (as seen in Scenarios 2 and 6), result in significant emissions reductions. However, the inclusion of global warming effects alone in Scenario 4 leads to varied impacts for cold and warm regions, sometimes resulting in increased emissions (Shenzhen and Shanghai) due to the changing energy demands for cooling and heating as the climate warms. Scenarios incorporating global warming effects help understand future performance and resilience but should not be considered as decarbonization strategies.

City-Specific Analysis

While Table 8 presents results limited to HVAC and DHW emissions, it offers a valuable metric for evaluating scenario effectiveness and comparing building performance across cooling-dominated and heating-dominated regions.

Beijing:

Beijing starts with baseline emissions ranging from 23.9 to 33.4 kg CO₂eq/m²·y. The worst-performing representative superblock is from cluster 2, as it has the highest shape factor, indicating that the buildings in this cluster are primarily low-rise buildings and terraced houses.

Scenario 2 (HVAC upgrades + PV panels) provides a significant reduction, reaching as low as - $69.9 \text{ kg CO}_2\text{eq/m}^2\text{-y}$. The representative block for cluster 2 performs exceptionally well because the total floor area of the buildings is relatively low, while there is sufficient space for rooftop PV panels. This results in a favourable PV panel area-to-total floor area ratio.

The representative block for Cluster 0 shows the lowest performance in Scenario 2, as it consists of high-rise buildings, resulting in a lower PV panel area per square meter compared to other clusters.

In Scenario 4, which applies global warming effects to the baseline building (without any additional energy efficiency measures), emissions decrease slightly. This suggests that global warming reduces emissions in heating-dominated regions, even though it increases cooling loads.

Scenarios 3 and 7, which include full upgrades, achieve further reductions, with emissions ranging from -7.0 to -79.7 kg CO₂eq/m²·y.

Harbin:

Harbin exhibits baseline emissions ranging from 25.2 to 29.4 kg $CO_2eq/m^2.y$. In Scenario 2 (HVAC + PV), emissions are reduced to as low as -12.6 kg $CO_2eq/m^2.y$, while Scenario 3, which applies all mitigation measures, achieves a further reduction to -21.1 kg $CO_2eq/m^2.y$. In contrast, Scenarios 4, 5, 6, and 7, which incorporate climate change effects, show smaller reductions due to global warming. Rising temperatures may reduce heating demands but simultaneously increase cooling needs, resulting in mixed outcomes for overall emissions.

The representative superblock of Cluster 0 has a higher median height of 26.34 meters, the lowest shape factor of 0.278, and an overall U-factor of 0.98 W/m²K, demonstrating better performance compared to other representative superblocks. However, after envelope improvements, nearly all representative clusters perform at similar levels. In Scenario 3 and Scenario 7, with all upgrades applied, the representative superblock for Cluster 1 achieves emissions of - 21.9 kg $\rm CO_2eq/m^2.y.$ This is due to its high shape factor, lower building height, and the advantage of a higher PV area-to-floor area ratio.

In Scenario 4, the baseline buildings are simulated under global warming conditions, and the carbon emissions of the superblocks are reduced due to rising temperatures. This is expected, considering that Harbin is located in a severely cold region.

Shanghai:

Shanghai has the lowest baseline emissions (17.3 to 23.1 kg $CO_2eq/m^2.y$), reflecting its milder climate. Scenario 2, which combines HVAC and PV, achieves reductions as low as -17.8 kg $CO_2eq/m^2.y$, while Scenarios 3 and 7 provide the most optimal reductions. Scenario 4, which incorporates global warming effects, results in an emissions increase for the representative superblock of Cluster 1 and a small increment for the representative superblock of Cluster 0.

At the baseline level, although the representative superblock for Cluster 0 has a lower U-factor, the median height of the representative superblock for Cluster 1 is 19.8 meters, which is higher

than that of Cluster 0 with a height of 10.4 meters. Additionally, Cluster 1 benefits from a more advantageous shape factor, ranging from 0.249 to 0.411.

In Scenarios 2, 3, 6, and 7, the disadvantage of the shape factor for the representative superblock of Cluster 0 becomes an advantage, as it achieves a higher PV area-to-floor area ratio, resulting in emissions as low as -18.6 kg CO₂eq/m².y.

Shenzhen:

Shenzhen, with baseline emissions ranging from 18.0 to 18.4 kg CO_2 eq/m².y, shows significant reductions from HVAC and PV panel upgrades. In Scenario 3, the representative superblock for Cluster 0 achieves the largest reduction, reaching -18.9 kg CO_2 eq/m².y, and Scenario 7 (full upgrades) leads to further improvements. This illustrates the effectiveness of HVAC and PV strategies in warm climates like Shenzhen, where higher temperatures and solar potential are both influential.

At the baseline level, both superblocks perform almost identically, but there is a significant performance difference in the scenarios where PV and HVAC upgrades are implemented. The median height of the representative superblock for Cluster 0 is 13 meters, while for Cluster 1, it is 24.3 meters. This difference is also reflected in the shape factors: the representative superblock for Cluster 0 has a shape factor of 3.59, whereas the representative superblock for Cluster 1 has a shape factor of 0.359. As a result, the superblock representative for Cluster 0 achieves the lowest carbon emissions, ranging from -15.8 to 18.9 kg CO₂eq/m².y.

The complete simulation results (including emissions from electric appliances and lighting) are provided in the Table 9. The results demonstrate that while the applied measures do not affect carbon emissions from electric appliances and lighting, they reveal that only the representative superblocks of Harbin Cluster 0 and Shenzhen Cluster 1 fail to meet either the net-zero or nearly-zero carbon emission thresholds, considering the average emissions at the superblock level. On the other hand, all other representative superblocks achieve either net-zero or nearly-zero carbon emissions. To further reduce emissions at this level, decarbonizing the electricity grid is necessary.

Table 9: Results of the representative superblock analysis under defined scenarios including electric appliances and lighting (kg CO₂eq/m².y).

Cluster	Location	Baseline	Scenario 1	Scenario 2	Scenario 3	Scenario 4	Scenario 5	Scenario 6	Scenario 7
0	Beijing	47.9	27.1	20.5	9.7	46.5	28.7	21.6	11.4
1	Beijing	46.3	26.7	-3.0	-13.4	45.2	28.2	-2.4	-12.0
2	Beijing	51.8	28.8	-50.8	-62.4	50.2	30.0	-50.8	-61.4
3	Beijing	42.2	27.6	10.9	3.0	41.8	29.0	12.0	4.5
0	Harbin	43.5	31.2	21.4	14.9	41.4	31.0	20.7	14.7
1	Harbin	47.7	30.5	5.7	-3.2	44.7	30.3	4.4	-3.6
2	Harbin	45.0	31.0	7.0	-0.3	42.8	30.9	6.2	-0.4
0	Shanghai	41.4	33.0	8.8	0.1	40.4	34.5	6.0	-0.2
1 -	Shanghai	35.7	30.0	18.0	12.1	36.0	31.9	17.1	12.6
0	Shenzhen	36.8	33.4	2.3	-1.1	42.3	38.0	6.2	1.6
1	Shenzhen	36.4	32.8	19.2	15.6	41.6	36.6	23.5	18.5

As shown in Table 9, most superblocks achieve nearly-zero or net-zero carbon emissions under Scenarios 2, 3, 6, and 7. However, deeper decarbonization of China's building stock will require additional measures, particularly the decarbonization of the electricity grid. Table 10 presents the carbon emissions of representative superblocks under a scenario with a 25% reduction in grid emissions. The carbon emission factor of the electricity grid is reduced from 0.6835 kgCO₂eq/kWh to 0.5126 kgCO₂eq/kWh. 25% decarbonization of electricity grid significantly reduces the carbon emission levels of the superblocks and at scenario 3 the average carbon emissions of all superblocks are below the nearly-zero

carbon emission threshold presented in the new zero-carbon. In addition, it is important to note that in scenarios involving reductions in grid carbon emissions, the carbon intensity of electricity decreases. Consequently, the emissions savings achieved by rooftop photovoltaic (PV) panels are also diminished, as the electricity they displace becomes less carbon-intensive due to grid decarbonization. The rest of the carbon emissions can be offset as suggested in the new zero-carbon building standard using methods such as carbon emissions trading and green power trading.

Table 10: Results of the representative superblock analysis under defined scenarios, including electric appliances and lighting, with a 25% decarbonized electricity grid (kg CO₂eq/m².y).

Cluste	r Location	Baseline	Scenario 1	Scenario 2	Scenario 3	Scenario 4	Scenario 5	Scenario 6	Scenario 7
0	Beijing	42.0	21.7	15.3	7.2	39.8	22.8	16.1	8.4
1	Beijing	40.5	21.4	-2.4	-10.1	38.6	22.4	-1.9	-9.1
2	Beijing	45,9	23.3	-38.2	-46.9	43.5	24.0	-38.2	-46.1
3	Beijing	36.4	22.2	8.1	2.2	35.3	23.1	8.9	3.3
0	Harbin	38.1	26.0	15.9	11.1	35.6	25.5	15.4	11.0
1	Harbin	42.3	25.4	4.2	-2.5	38.9	24.8	3.2	-2.8
2	Harbin	39.6	25.9	5.2	-0.3	36.9	25.3	4.6	-0.4
0	Shanghai	32.9	26.5	6.5	0.0	32.1	27.6	4.4	-0.3
1	Shanghai	28.3	24.1	13.4	9.0	28.6	25.5	12.7	9.3
0	Shenzhen	29.3	26.8	1.6	-0.9	33.4	30.2	4.5	1.1
1	Shenzhen	29.0	26.3	14.3	11.6	32.9	29.2	17.6	13.8

To reflect anticipated reductions in carbon intensity due to grid decarbonization and to further lower emissions from the building stock, a 50% decrease in the electricity grid's emission factor was assumed. The results indicate a significant reduction in both current and projected carbon emissions. Nevertheless, even after this adjustment resulting in an emission factor of 0.34175 kgCO₂eq/kWh the associated emissions remain relatively high and suggest additional potential for decarbonization. Simulation results assuming a 50% decarbonization of the electricity grid are presented in Table 11.

In the final scenario for grid emission reduction, the carbon intensity of the electricity grid is assumed to decrease by 90%, with the results presented in Table 12. As expected, carbon emissions are significantly reduced. However, to achieve net-zero emission targets, the remaining emissions must be offset, or additional photovoltaic (PV) panels need to be integrated into buildings.

Table 11: Results of the representative superblock analysis under defined scenarios, including electric appliances and lighting, with a 50% decarbonized electricity grid (kg CO₂eq/m².y).

luste	r Location	Baseline	Scenario 1	Scenario 2	Scenario 3	Scenario 4	Scenario 5	Scenario 6	Scenario
0	Beijing	36.2	16.5	10,2	4.8	33.2	17.0	10.7	5.6
1	Beijing	34.8	16.1	-1.6	-6.8	32.2	16.7	-1.3	-6.0
2	Beijing	40.1	18.0	-25.5	-31.3	37.1	18.1	-25.5	-30.7
3	Beijing	30.7	16.9	5.4	1.4	28.8	17.2	5.9	2.2
0	Harbin	32.8	21.0	10.6	7.4	29.8	20.1	10.3	7.3
1	Harbin	37.1	20.4	2.8	-1.7	33.2	19.5	2.1	-1.8
2	Harbin	34.3	20.8	3,4	-0.2	31.2	19.9	3.0	-0.3
0	Shanghai	24.4	20.2	4.3	0.0	23.9	20.9	3.0	-0.2
1	Shanghai	21.1	18.3	8.9	6.0	21.3	19.2	8.5	6.2
0	Shenzhen	21.9	20.2	1.1	-0.6	24.7	22.5	3.0	0.8
1	Shenzhen	21.7	19.9	9.5	7.7	24.3	21.8	11.7	9.2

Table 12: Results of the representative superblock analysis under defined scenarios, including electric appliances and lighting, with a 90% decarbonized electricity grid (kg CO₂eq/m².y).

Cluster	Location	Baseline	Scenario 1	Scenario 2	Scenario 3	Scenario 4	Scenario 5	Scenario 6	Scenario 7
0	Beijing	26.8	8,0	2.0	1.0	22.6	7.7	2.1	1.1
1	Beijing	25.6	7.8	-0.3	-1.4	21.9	7.5	-0.3	-1.2
2	Beijing	30.9	9.5	-5.1	-6.3	26.7	8.7	-5.1	-6.1
3	Beijing	21.5	8.4	1.1	0.3	18.5	7.9	1.2	0,4
0	Harbin	24.3	13.0	2.1	1.5	20.6	11.5	2.1	1.5
1	Harbin	28.6	12.4	0.6	-0.3	24.0	10.9	0.4	-0.4
2	Harbin	25.9	12.8	0.7	0.0	21.9	11.2	0.6	-0.1
0	Shanghai	10.9	10.1	0.9	0.0	10.7	10.1	0.6	0.0
1	Shanghai	9.6	9.0	1.8	1.2	9.6	9.1	1.7	1.2
0	Shenzhen	10.2	9,8	0.2	-0.1	10.6	10.2	0.6	0.2
1	Shenzhen	10.1	9,7	1.9	1,5	10.5	10.0	2.3	1.8

2.5 Work Package E and Work Package F — Upscaling Process and Scenario Analysis

In this phase of the project, the simulation results and the model produced during the clustering stage are used to predict the carbon emissions of a zone approximately 1 km² in size. This part of the study aims to demonstrate and test the upscaling potential of the implemented methodology. For this purpose, a zone is selected from each city. The zone selection was conducted manually, again, due to missing data, particularly incomplete building footprint and block data. While missing building footprint areas can be manually reconstructed, street block data is obtained from Long et al. (2019) and cannot be generated for locations where it is unavailable. In the case of Shenzhen, only a few zones have an acceptable amount of data, and even these require some manual completion for building footprint areas. For the other cities, there is also a limited amount of data. Due to these constraints, the selection of the upscaling zone is restricted to manual selection, making it a necessary step in the process.

Using GIS analysis, the layers of street blocks and building footprints (with information on height and archetype), consisting of polygons, are combined. The age for the entire zone is assumed to be uniform due to a lack of continuous age data. Using the age data samples provided by CABR, the data point closest to the selected zone is identified, and the age of the buildings in the selected zone is assumed to be the same. Next, the three parameters – density, shape factor, and overall U-factor – are calculated for each superblock, and the calculated values are assigned to the corresponding superblock polygons. Using the trained k-means clustering model, the cluster to which each superblock belongs is predicted and assigned to its respective polygon.

After determining the cluster of each superblock, the results presented in Table 8, Table 9, Table 10, Table 11, Table 12 are used to predict the carbon emissions of each superblock in the selected area at the baseline level and under different scenarios, including global warming and combinations of upgrades as previously presented in Table 7.

2.5.1.Beijing - Upscaling

The selected zone presented in

Figure 18 and superblock cluster representation for the upscaling zone is presented in Figure 19. It is located at 39.92°, 116.46°, very close to the city centre and comprises 372 buildings with an average height of 15.57 meters. The total floor area of the zone is 1,696,147 m², with a total building footprint area of 263,897 m². The building archetypes in the zone are diverse, including 81 high-rise slab

buildings, 11 high-rise towers, 169 low-rise buildings, 109 terraced houses, and 2 commercial buildings with footprint areas larger than 3,000 m². This mix of building types and heights provides a representative sample for testing the upscaling methodology.



Figure 18: Selected upscaling zone for Beijing

Figure 19 presents the superblock cluster representation for the upscaling zone in Beijing. A trained k-means model was utilized to classify each superblock within the upscaling zone. The zone is divided into 67 superblocks, consisting of 8 in cluster 0, 5 in cluster 2, 52 in cluster 3, and 2 non-residential superblocks. The majority of the superblocks are classified as cluster 3; therefore, the upscaling zone overall has a high U-factor, moderate density, and moderate shape factor. Superblocks classified as cluster 0 have the highest density and the lowest shape factor among all clusters. In contrast, cluster 2 has the lowest density and, correspondingly, the highest shape factor.

Based on the clusters determined for each superblock, carbon emissions are predicted using the values presented in Table 8, Table 9, Table 10, Table 11, and Table 12. The values obtained from the table are multiplied by the total floor area of buildings in the corresponding superblock, and this calculation is performed for all superblocks within the upscaling zone. The total carbon emissions calculated are then divided by the total floor area to determine the carbon emissions per square meter of building floor area and presented in

Table 13.

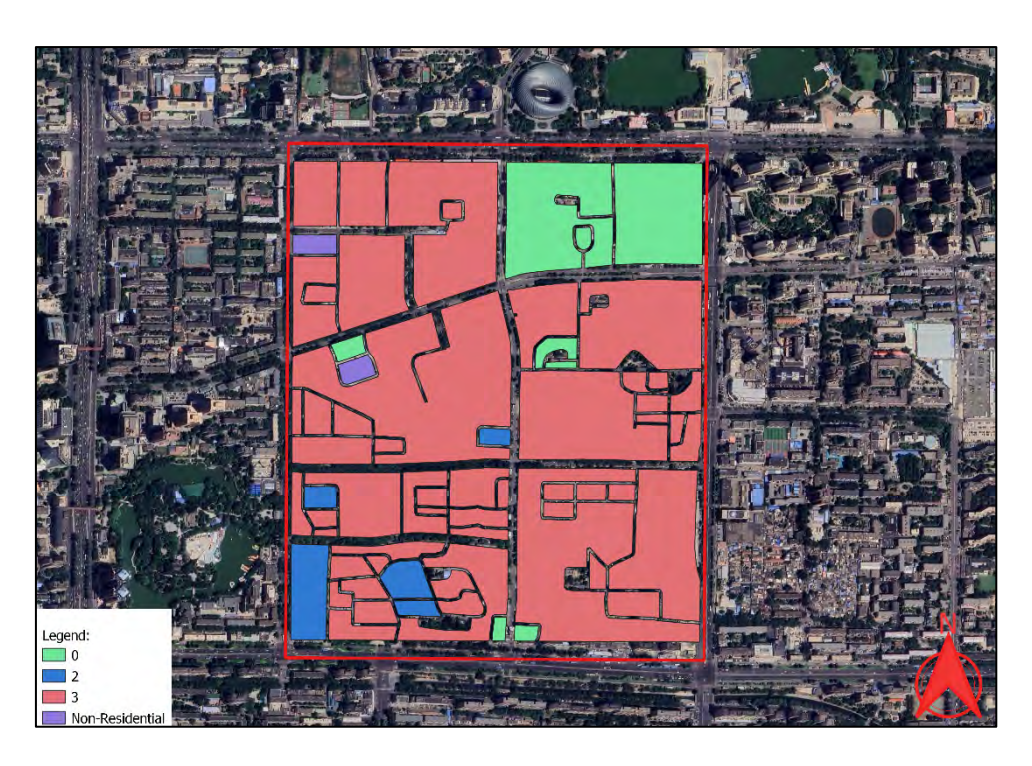


Figure 19: Beijing superblock clusters for upscaling zone

Table 13: Beijing carbon emissions for upscaling zone (kg CO₂eg/m².y)

	Baseline	Scenario 1	Scenario 2	Scenario 3	Scenario 4	Scenario 5	Scenario 6	Scenario 7
HVAC and DHW	25.69	9.14	-5.65	-14.46	24.98	10.58	-4.58	-12.93
All activities	44.05	27.5	12.71	3.9	43.34	28.94	13.78	5.43
All activities + 25% grid decarb.	38.19	22.07	9.45	2.86	36.75	23.03	10.24	3.99
All activities + 50% grid decarb.	32.46	16.80	6.30	1.86	30.22	17.16	6.79	2.66
All activities + 90% grid decarb.	23.20	8.30	1.26	0.40	19.83	7.85	1.36	0.50

Commercial buildings contribute only to the density value, as their shading effect is considered. However, their shape and U-factors are not calculated or taken into account. When only the HVAC and DHW considered upscaling zone achieves net-zero carbon emissions in Scenarios 2 and 3. Additionally, with the influence of global warming, it also reaches net zero in Scenarios 6 and 7. However, with inclusion of carbon emissions sourced by electric appliances and lighting the carbon emission levels increase over net-zero level but stays under nearly zero-carbon threshold defined in the zero-carbon building standard. However, with the inclusion of carbon emissions from electric appliances and lighting, the carbon emission levels rise above the net-zero threshold but remain below the nearly zero-carbon threshold defined in the zero-carbon building standard.

Focusing exclusively on HVAC and hot water systems, baseline emissions show minimal sensitivity to global warming (-3.5%, 25.69 to 24.98 kg CO₂eq/m²·yr). Passive measures transform this relationship: Scenario 1 cuts space conditioning and water heating emissions by 64% (25.69 to 9.14). When climate

change interacts with these measures (Scenario 5), the combined systems achieve a 57.6% reduction versus warmed baseline levels (24.98 to 10.58).

The increase in carbon emissions between Scenario 1 and Scenario 5 can be attributed to two main factors. First, the improvement in the building envelope significantly reduces heating loads, and Scenario 1 shows a major reduction in carbon emissions compared to the baseline. However, with the introduction of global warming, the reduction in carbon emissions due to warming and the decrease in heating loads are outweighed by the increase in cooling loads caused by rising temperatures. The second factor is that the cooling systems in the building rely on electricity, which has a carbon emission rate nearly three times higher than that of natural gas. With the introduction of a 90% decarbonization scenario for the electricity grid, carbon emissions decrease from Scenario 1 to Scenario 5, as the carbon intensity of electricity becomes lower than that of natural gas.

2.5.2. Harbin - upscaling

The selected zone illustrated in

Figure 20 and Figure 21 consists of 209 buildings with an average height of 17.49 meters. The total floor area of the zone is 1,727,446 m², with a total footprint area of 238,983.78 m². The building archetypes in the zone are varied, including 64 high-rise slab buildings, 123 low-rise buildings, 13 terraced houses, and 9 commercial buildings, all with footprint areas larger than 3,000 m². This diverse mix of building types and heights offers a representative sample for evaluating the upscaling methodology.

Figure 21 presents the superblock clusters for the upscaling zone in Harbin. The upscaling zone is located at 45.72°, 126.64°, situated within the urban area. A trained k-Means model was utilized to classify each superblock within the upscaling zone. The zone is divided into 36 superblocks, consisting of 7 in cluster 0, 27 in cluster 2, and 2 non-residential superblocks.



Figure 20: Selected upscaling zone for Harbin

The majority of the superblocks are classified as cluster 2; therefore, the upscaling zone overall has a high U-factor, low density, and the highest shape factor, indicating that the buildings are generally low-rise with high U-factor. Superblocks classified as cluster 0 have the highest density and the lowest shape factor among all clusters, along with a moderate U-factor. In contrast, cluster 2 has the lowest density and, correspondingly, the highest shape factor.



Figure 21: Harbin superblock clusters for upscaling zone

The abovementioned calculation is done for the Harbin upscaling zone to calculate carbon emission per square meter of the building within the upscaling zone. The results are presented in Table 14.

Table 14: Harbin Carbon Emissions for Upscaling Zone (kg CO₂eq/m².y)

	Baseline	Scenario						
		1	2	3	4	5	6	7
HVAC and DHW	26.38	12.65	-9.09	-16.23	24.26	12.56	-9.87	-16.36
All activities	44.74	31.01	9.27	2.13	42.62	30.92	8.49	2.00
All activities + 25% grid decarb.	39.36	25.92	6.88	1.49	36.70	25.33	6.30	1.39
All activities + 50% grid decarb.	34.06	20.83	4.53	1.00	30.98	19.93	4.15	0.90
All activities + 90% grid decarb.	25.65	12.83	0.92	0.24	21.70	11.25	0.84	0.15

For HVAC and domestic hot water (DHW) systems in Harbin, global warming moderately reduces baseline emissions by 8.0% (26.38 to 24.26 kg $CO_2eq/m^2\cdot yr$). These HVAC/DHW systems respond dramatically to passive measures: Scenario 1's shading and envelope improvements achieve a 52% reduction (26.38 to 12.65 kg $CO_2eq/m^2\cdot yr$). When global warming combines with passive strategies (Scenario 5), the HVAC/DHW systems show further improvement (24.26 to 12.56 kg $CO_2eq/m^2\cdot yr$), representing a 48.2% reduction from climate-adjusted baseline HVAC/DHW emissions.

For HVAC and domestic hot water (DHW) systems, Scenarios 1 and 5 (passive measures ± global warming) show minimal performance differences. While warming reduces heating loads, the concurrent cooling load increase partially offsets emission gains. Notably, these cooling systems use grid electricity

with a carbon intensity triple that of natural gas (consistent with Beijing's conditions). In contrast, Scenarios 2, 3, 6 and 7 demonstrate transformative HVAC/DHW emission reductions through PV and heat pump integration: Scenario 3 achieves -16.23 kg CO_2 eq/m²·yr, while Scenario 7 reaches -16.36 kg CO_2 eq/m²·yr, proving carbon-negative operation is attainable in the upscaling zone.

When all activities are considered, carbon emissions in Scenarios 3 and 7 decrease to 2.13 kg CO_2 eq/m²·y and 2.00 kg CO_2 eq/m²·y, respectively. To reach net-zero, these remaining emissions would need to be offset or further reduced through the integration of additional PV panels. On the other hand, with a 90% reduction in the carbon intensity of the electricity grid, the carbon emissions in the upscaling zone are reduced to almost net-zero levels (0.24 kg CO_2 eq/m²·y).

2.5.3. Shanghai - upscaling

The selected zone depicted in Figure 22 encompasses 427 buildings with an average height of 25.64 meters. The total floor area of the zone is 2,873,263 m², with a total footprint area of 269,576 m². The building archetypes in the zone are diverse, including 66 high-rise slab buildings, 62 high-rise towers, 242 low-rise buildings, 53 terraced houses, and 4 commercial buildings, all of which have footprint areas larger than 3,000 m². This varied combination of building types and heights provides a comprehensive and representative sample for testing the upscaling methodology.



Figure 22: Selected upscaling zone for Shanghai

Figure 23 presents the superblock clusters for the upscaling zone in Shanghai. The upscaling zone is located at 31.21°, 121.38°, situated within the urban area. A trained k-means model was utilized to classify each superblock within the upscaling zone. The zone is divided into 33 superblocks, consisting of 9 in cluster 0 and 24 in cluster 1.

The majority of the superblocks are classified as cluster 1; therefore, the upscaling zone overall has a higher density, lower shape factor, and higher U-factor compared to cluster 0, indicating that the buildings are generally more compact but have poor envelope performance. Superblocks classified as cluster 0 have lower density, a higher shape factor, and a lower U-factor, representing a more dispersed urban form with comparatively better envelope performance.

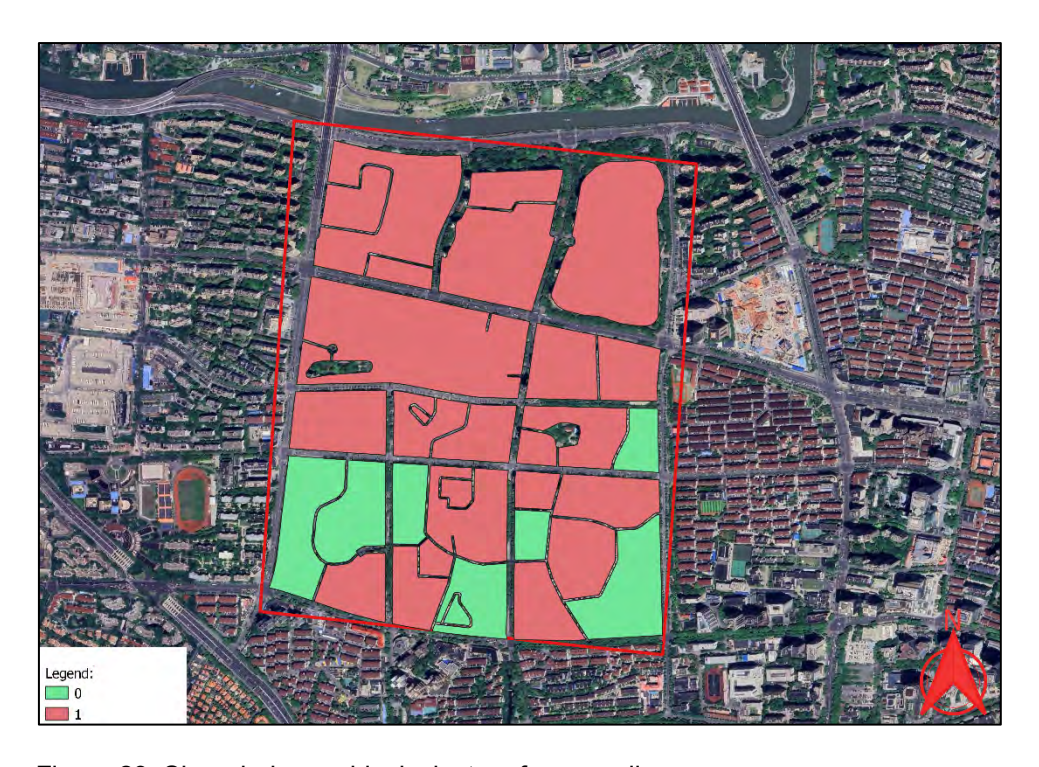


Figure 23: Shanghai superblock clusters for upscaling zone

The average carbon emissions per square meter for the upscaling zone are calculated and presented in Table 15. The baseline average HVAC and DHW carbon emission for the upscaling zone is 17.95 kg $\rm CO_2 eq/m^2.y.$ With the application of passive measures in Scenario 1, it is reduced to 11.97 kg $\rm CO_2 eq/m^2.y.$ representing a 33.3% reduction. In Scenario 2, with the addition of proposed HVAC systems, and in Scenario 3, with the implementation of envelope improvements, HVAC systems, and PV panels, the average carbon emissions are reduced below zero, reaching negative values.

Table 15: Shanghai Carbon Emissions for Upscaling Zone (kg CO₂eq/m².y)

	Baseline	Scenario 1	Scenario 2	Scenario 3	Scenario 4	Scenario 5	Scenario 6	Scenario 7
HVAC and DHW	17.95	11.97	-1.35	-7.56	18.15	13.80	-2.50	-7.20
All activities	36.31	30.33	17.01	10.8	36.51	32.16	15.86	11.16
All activities + 25% grid decarb.	28.81	24.36	12.64	8.01	28.99	25.73	11.79	8.24
All activities + 50% grid decarb.	21.46	18.51	8.39	5.34	21.59	19.39	7.89	5.49
All activities + 90% grid decarb.	9.74	9.12	1.70	1.07	9.72	9.21	1.58	1.07

Following envelope improvements in Scenario 1, the upscaling zone's buildings transition to a strongly cooling-dominated regime. When global warming is introduced (Scenario 5), average HVAC and DHW system emissions rise from 11.97 to 13.80 kg CO₂eq/m²·y (+15.3%). Conversely, Scenario 2's heating-dominated buildings show opposite trends - with global warming effects (Scenario 6), the HVAC/DHW systems achieve net-negative emissions of -2.50 kg CO₂eq/m²·y.

The HVAC and DHW emission patterns between Scenarios 3 and 7 mirror those between Scenarios 1 and 5. When all measures are implemented (Scenario 3), the upscaling zone's HVAC and DHW systems transition to a net cooling-dominated state. Consequently, global warming causes a marginal increase in these systems' emissions from -7.56 to -7.20 kg CO₂eq/m²·y.

When all activities are considered under the current grid carbon intensity, the carbon emissions of the upscale zone in Scenarios 3 and 7 fall below the nearly zero-carbon threshold defined in the new Zero-Carbon Building Standard. As the carbon intensity of the grid decreases, building performance improves, and emissions are further reduced. The remaining emissions should either be offset or covered by the integration of additional PV panels.

2.5.4. Shenzhen - upscaling

The selected zone presented in Figure 24 comprises 248 buildings with an average height of 35.50 meters. The total floor area of the zone is 5,445,756 m², with a total footprint area of 304,579 m². The building archetypes in the zone are diverse, including 141 high-rise slab buildings, 25 high-rise towers, 58 low-rise buildings, 9 terraced houses, and 15 commercial buildings, all of which have footprint areas larger than 3,000 m². This mix of building types and heights, particularly the dominance of high-rise structures, provides a robust and representative sample for evaluating the upscaling methodology.



Figure 24: Selected upscaling zone for Shenzhen

Figure 25 presents the superblock clusters for the upscaling zone in Shenzhen. The upscaling zone is located at 22.54696°, 114.08669°, situated within the urban area. A trained k-Means model was utilized to classify each superblock within the upscaling zone. The zone is divided into 51 superblocks, consisting of 7 in Cluster 0, 36 in Cluster 1, and 8 non-residential superblocks.

The majority of the superblocks within the upscaling zone are classified as Cluster 1, indicating that most of the buildings have higher density, a lower shape factor, and a higher U-factor, which reflects a lower level of envelope performance. On the other hand, 8 superblocks are classified as non-residential, meaning these blocks contain no residential buildings and are therefore excluded from the predictions. Superblocks classified as Cluster 0 exhibit lower density, a higher shape factor, and a lower U-factor, representing a more dispersed urban form with comparatively better envelope performance.

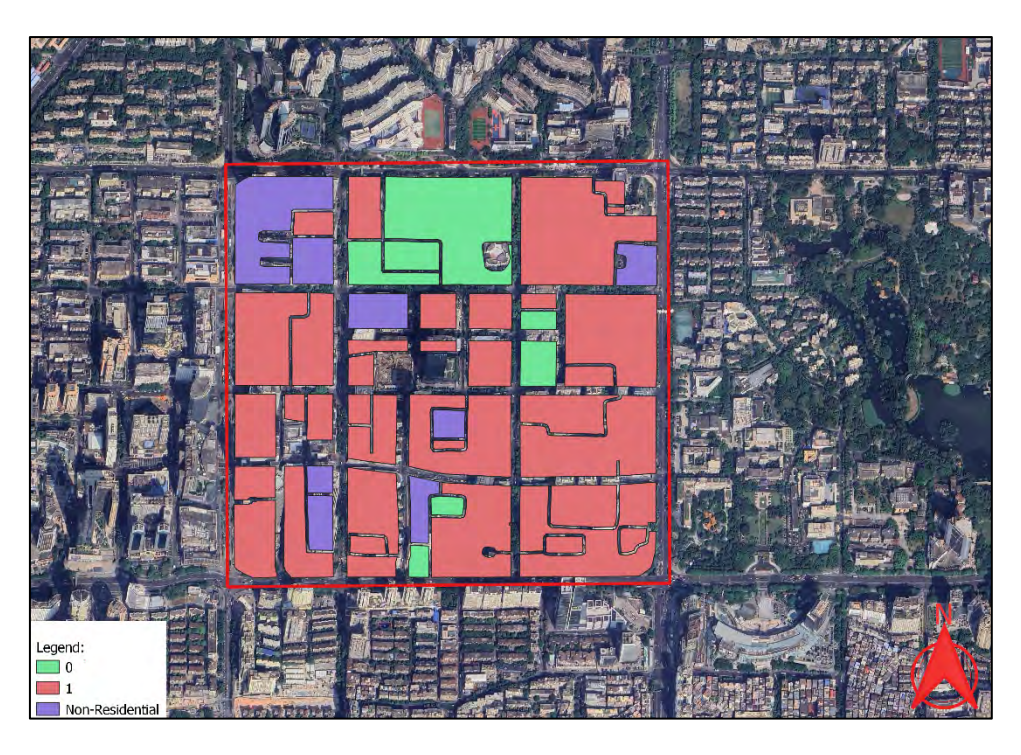


Figure 25: Shenzhen Superblock Clusters for Upscaling Zone

The overall average carbon emissions per square meter for the upscaling zone are calculated and presented in Table 16.

The baseline emissions from space conditioning and domestic hot water systems (HVAC+DHW) in the upscaling zone measure 18.03 kg CO_2 eq/m²·yr. With envelope improvements and shading (Scenario 1), this drops by 20% to 14.44 kg CO_2 eq/m²·yr. Scenario 2's introduction of PV and heat pumps achieves net-negative emissions for these systems. The comprehensive measures in Scenario 3 further reduce emissions to -3.71 kg CO_2 eq/m²·yr.

Table 16: Shenzhen Carbon Emissions for Upscaling Zone (kg CO₂eq/m².y)

	Baseline	Scenario 1	Scenario 2	Scenario 3	Scenario 4	Scenario 5	Scenario 6	Scenario 7
HVAC and DHW	18.03	14.44	-0.15	-3.71	23.30	18.36	4.20	-0.80
All activities	36.39	32.8	18.21	14.65	41.66	36.72	22.56	17.56
All activities + 25% grid decarb.	29.02	26.33	13.58	10.89	32.93	29.26	16.86	13.08
All activities + 50% grid decarb.	21.71	19.92	9.03	7.23	24.32	21.84	11.21	8.73
All activities + 90% grid decarb.	10.11	9.71	1.80	1.41	10.51	10.01	2.20	1.71

As a cooling-dominated region with a hot climate, Shenzhen experiences increased cooling loads under global warming, significantly raising the upscaling zone's emissions. Space conditioning and hot water system emissions rise from 18.03 to 23.30 kg CO₂eq/m²·yr (+29.2%) in the baseline scenario. With passive measures (Scenario 1), this increase moderates to 18.36 kg CO₂eq/m²·yr (+27.1% from original

baseline). While Scenario 6 loses its negative emission status (rising to 4.20 kg CO₂eq/m²·yr), Scenario 7 maintains near-neutral emissions at -0.80 kg CO₂eq/m²·yr.

Decarbonization of the electricity grid also helps the upscaling zone achieve carbon emissions below the nearly zero-carbon threshold defined in the Zero-Carbon Building Standard. Further reductions in the grid's carbon intensity significantly lower emissions, and with a 90% reduction in Scenario 3, carbon emissions decrease to 1.41 kg CO₂eq/m²·y.

3 Conclusions

In this study, the assumption that the upscaling method based on superblocks would be an effective approach to quantify the impact of the new zero-carbon standard to be published by the Chinese authorities was tested. The results presented in work packages E and F demonstrated that the methodology indeed allows for a quick projection of current emissions and emissions reductions under the assumption of different emission reduction pathways. The proposed methodology was developed and tested on four upscaling zones in distinct climate regions under different scenarios and successfully quantified the carbon emission reductions and the current performance of the buildings at the urban scale. The project also demonstrated that the quality of the results heavily depends on the completeness and availability of the data.

The conducted research allows to give the following answers to the questions raised at the beginning of the project:

- Reaching zero emission standard: With the carbon intensity of 0.6835 kgCO₂eq/kWh zero emission standard can only be reached for low-rise buildings with a high coverage of roof-top PV. For reaching the standard, for all other building types, a decarbonization of the electricity grid is an absolute requirement as the carbon emissions stemming from the electricity demand of appliances alone often-time exceed the zero-emission threshold set by the standard.
- Assessing the energy performance of existing residential buildings: The emission intensity of the current building stock is simulated at both the building level (WP-B) and superblock level (WP-D and WP-E). The results have shown that the current building stock generally does not reach the nearly zero-emission thresholds defined in the new zero-carbon buildings standard. Additionally, the baseline performance of each building archetype inspected for different climates and age classes (a total of 48 buildings) is presented in the study.

In heating-dominated regions (e.g., Beijing, Harbin), buildings exhibit high heating energy demands due to cold winters. For example, building-level baseline simulations showed that buildings in Beijing and Harbin have higher heating loads, with carbon emissions ranging from 31.3 to 74.2 kg CO₂eq/m²/yr and 37.1 to 79.4 kg CO₂/m²/yr, respectively. In the cooling-dominated regions (e.g., Shenzhen), baseline emissions are ranging from 38.2 to 42.0 kg CO₂/m²/yr. In more balanced climates (e.g., Shanghai), buildings showed a more balanced heating and cooling demand, with baseline emissions ranging from 45.0 to 59.3 kg CO₂/m²/yr.

Overall, the energy performance of existing buildings is highly dependent on climate conditions, building archetypes, and construction standards. Particularly, terraced houses and low-rise structures tend to have poorer energy performance compared to high-rise buildings due to the increased shape factor. In addition, the age of the building is a major factor that influences the performance of the building, as in Shenzhen, the building stock is comparatively new and performs better than older building stocks in other regions.

Quantifying the impact of Zero-Carbon Standards: With the implementation of the new performance-based zero-carbon standard being prepared by the Chinese authorities, the net emissions of the building stock are aimed to be reduced to net-zero or even reach to the net-negative carbon emissions. The main contribution of this project is to determine what it takes to achieve

this new ZEB building standard and estimate its CO₂ emission reduction potential and impact with reference to a baseline. Considering the baseline carbon emissions of the upscaling zones in Beijing (44.05 kg CO₂eq/m².y), Harbin (44.74 kg CO₂eq/m².y), Shanghai (36.31 kg CO₂eq/m².y), and Shenzhen (36.39 kg CO₂eq/m².y), these values are first reduced to the nearly zero-energy building threshold and then offset to zero emissions with the introduction of the new standard.

The total carbon reduction impact has been calculated for the upscaling zones, each measuring 1 km², using the current grid carbon emission intensity. In Beijing, the emission reduction potential for Scenario 3 compared to the baseline is 68,100 tons CO_2 eq/year. For Harbin, it is 73,606 tons CO_2 eq/year, while in Shanghai, it is 73,296 tons CO_2 eq/year. The upscaling zone in Shenzhen shows the highest reduction potential, with a 118,390 tons CO_2 eq/year for Scenario 3.

• Identifying effective retrofit strategies: In cold and severely cold regions, envelope improvements significantly enhance performance, while in hot climate regions, shading systems play a crucial role in reducing cooling loads. However, envelope upgrades have a relatively limited impact in hot climates compared to shading measures. Additionally, due to the impact of global warming, it becomes even more challenging for Shenzhen to meet zero-emission goals. Renewable energy measures are essential to reduce carbon emissions and achieve the required nearly-zero or zero-emission levels. Generally, HVAC improvements and the addition of PV panels have a significant impact across all climate regions, reducing emissions to a net negative level especially in low-rise buildings and upscaling zones with a low average height.

To sum up, the most effective retrofit strategies vary by climate zone. In heating-dominated regions like Beijing and Harbin, envelope upgrades such as insulation improvements for walls, roofs, and floors, along with window upgrades, significantly reduce heating demands. HVAC improvements, particularly transitioning from gas-based heating systems to air-source heat pumps (ASHPs), result in substantial emission reductions, even though current emission intensities for electricity in the Chinese electricity grid are currently very high. Additionally, in regions with sufficient solar potential, integrating photovoltaic (PV) systems further reduces emissions. In cooling-dominated regions like Shenzhen, passive measures such as shading systems are critical for reducing cooling loads. Upgrading cooling systems to more efficient heat pumps and integrating PV panels are essential for achieving emission targets, while envelope improvements are less impactful than in heating-dominated regions, but still contribute to overall energy savings. In balanced climates like Shanghai, a combination of envelope upgrades, HVAC improvements, and PV integration proves most effective, as both heating and cooling demands need to be addressed. Overall, the most impactful strategies are those that combine passive measures (e.g., insulation, shading) with active systems (e.g., heat pumps, PV panels), tailored to the specific climatic conditions of each region.

- Comparing Simulation Scales: The study shows that superblock-level analysis offers a more realistic assessment of energy performance compared to a building-level analysis by also considering shading along with the effects it has on heating and cooling loads and PV yields. It further improves the reliability of scaling-up retrofit strategies, leading to more effective planning and implementation.
- Identifying prioritized zones for retrofitting: The proposed framework effectively classifies superblocks within large urban areas using three simple parameters: density, overall shape factor, and overall U-factor. These parameters allow zones to be easily partitioned into clusters, enabling the determination of current or baseline carbon emissions for the region. The framework identified superblocks with high emissions, particularly those featuring older, low-rise buildings or those with poor insulation levels, as priority areas for retrofits. Additionally, superblocks with low density and high shape factors were flagged for targeted interventions due to their higher energy demands resulting from inefficient building layouts.

4 Outlook

Despite the progress made in this project, there are remaining areas for improvement and extension in the analysis of building performance in the context of China:

- Data Availability & Resolution: The limited availability of data on building footprints, superblocks, and building age, coupled with the low resolution of height data, constrained the full potential of the framework. With support from Chinese authorities and access to high-quality data, the framework could be tested on a larger scale with much greater accuracy.
- Building Typology: This study focused exclusively on residential buildings. However, commercial buildings, such as office towers, have significantly higher energy demands and should be incorporated into future analyses to provide a more comprehensive understanding of energy performance and operational carbon emissions.
- Photovoltaic (PV) Integration: Currently, PV panels were only considered on the rooftops of residential buildings. For future research—particularly in high-rise developments—integrating PV panels on building facades should be explored to achieve net-zero or even net-negative carbon emissions. Even retrofit options with thin film PV on existing façade panels could offer an interesting way for reduction of operational emissions.
- Electrification & Energy Sources: The scenario analysis targeted building electrification as a strategy for reducing carbon emissions. However, China's continued reliance on fossil fuels for electricity generation negatively impacts the overall emissions performance of residential buildings with the carbon intensity (kgCO2eq/kWh) of the electricity grid being currently three times higher than the one of natural gas. Future studies should consider countrywide changes in the energy mix and the role of renewables in reducing emissions. While there is no way around the phase-out of fossil fuels for reaching the zero-emission target, the electricity supply will be gradually decarbonized with the integration of more renewable generation sources. To be able to achieve zero carbon emission in the building sector a strong decarbonization of the electricity sector is mandatory. To be able to achieve zero carbon emission in the building sector a strong decarbonization of the electricity sector is mandatory.
- Life-cycle emissions: This study focused on operational emission reductions based on the
 thresholds defined in the new national zero emission standard. For the goal to decarbonize the
 building sector the embodied emissions play an equally important part as the operational ones.
 In the sense of a holistic carbon emission perspective, the full life cycle emissions would need
 to be considered. This would further inform the decision making in respect to choosing intervention measures such as building retrofit vs. replacement and lead to balancing of retrofit
 measures such as the addition of additional insulation in the envelope vs, improving the efficiency of HVAC equipment.
- Net zero energy/emission perspective: The net zero energy assumptions present a simplification in the analysis of the building energy performance that was adopted in this project. With this, it assumes that the integration of renewable electricity generation such as PV will lead to a reduction in carbon emissions proportional to the electricity it produces in the course of the year. Thus, the excess electricity that cannot absorbed at the building level will be sold back to the grid and replace another, generation capacity. This assumption is justified as long as little renewable generation capacity is included in the grid but would have to be refined in case of large renewable capacities would generate excess supply, e.g. during peak hours in summer.

5 Publications and other communications

Accepted - Yigit, S., Mahecha Zambrano, J., & Baldini, L. (2025). A GIS and bottom-up simulation-based framework to assess the role of zero-emission building standards in achieving low-carbon goals: Insights from a case study for China. Third International Conference on Construction, Energy, Environment and Sustainability - CEES 2025, Bari, Italy, June 11-13, 2025.

6 References

An, J., Wu, Y., Gui, C., & Yan, D. (2023). Chinese prototype building models for simulating the energy performance of the nationwide building stock. *Building Simulation*, *16*(8), 1559–1582. https://doi.org/10.1007/s12273-023-1058-5

Braun, M., Stetz, T., Bründlinger, R., Mayr, C., Ogimoto, K., Hatta, H., Kobayashi, H., Kroposki, B., Mather, B., Coddington, M., Lynn, K., Graditi, G., Woyte, A., & MacGill, I. (2012). Is the distribution grid ready to accept large-scale photovoltaic deployment? State of the art, progress, and future prospects. *Progress in Photovoltaics: Research and Applications*, *20*(6), 681–697. https://doi.org/10.1002/pip.1204

Dai, B., Cao, Y., Liu, S., Ji, Y., Sun, Z., Xu, T., Zhang, P., & Nian, V. (2022). Annual energetic evaluation of multi-stage dedicated mechanical subcooling carbon dioxide supermarket refrigeration system in different climate regions of China using genetic algorithm. *Journal of Cleaner Production*, 333, 130119. https://doi.org/10.1016/j.jclepro.2021.130119

Deng, Z., Javanroodi, K., Nik, V. M., & Chen, Y. (2023). Using urban building energy modeling to quantify the energy performance of residential buildings under climate change. *Building Simulation*, *16*(9), 1629–1643. https://doi.org/10.1007/s12273-023-1032-2

Eggimann, S., Vulic, N., Rüdisüli, M., Mutschler, R., Orehounig, K., & Sulzer, M. (2022). Spatiotemporal upscaling errors of building stock clustering for energy demand simulation. *Energy and Buildings*, 258, 111844. https://doi.org/10.1016/j.enbuild.2022.111844

Eom, J., Clarke, L., Kim, S. H., Kyle, P., & Patel, P. (2012). China's building energy demand: Long-term implications from a detailed assessment. *Energy*, *46*(1), 405–419. https://doi.org/10.1016/j.energy.2012.08.009

Esch, T., Brzoska, E., Dech, S., Leutner, B., Palacios-Lopez, D., Metz-Marconcini, A., Marconcini, M., Roth, A., & Zeidler, J. (2022). World Settlement Footprint 3D - A first three-dimensional survey of the global building stock. *Remote Sensing of Environment*, 270, 112877. https://doi.org/10.1016/j.rse.2021.112877

Gan, Y., El-Houjeiri, H. M., Badahdah, A., Lu, Z., Cai, H., Przesmitzki, S., & Wang, M. (2020). Carbon footprint of global natural gas supplies to China. *Nature Communications*, *11*(1), 1–9.

Geng, J., Wang, J., Huang, J., Zhou, D., Bai, J., Wang, J., Zhang, H., Duan, H., & Zhang, W. (2022). Quantification of the carbon emission of urban residential buildings: The case of the Greater Bay Area cities in China. *Environmental Impact Assessment Review*, *95*, 106775. https://doi.org/10.1016/j.eiar.2022.106775

Geofabrik. (2024, January 15). *Download OpenStreetMap data for this region: China*. Geofabrik. https://download.geofabrik.de/asia/china.html

Güneralp, B., & Seto, K. C. (2008). Environmental impacts of urban growth from an integrated dynamic perspective: A case study of Shenzhen, South China. *Global Environmental Change*, *18*(4), 720–735. https://doi.org/10.1016/j.gloenvcha.2008.07.004

- Guo, S., Yan, D., Hu, S., & Zhang, Y. (2021). Modelling building energy consumption in China under different future scenarios. *Energy*, 214, 119063. https://doi.org/10.1016/j.energy.2020.119063
- Housing, M. of, & China (MoHURD), U.-R. D. of P. (2019). *Technical Standard for Nearly Zero Energy Buildings*. China Building Industry Press.
- Huang, B., Xing, K., Ness, D., Liao, L., Huang, K., Xie, P., & Huang, J. (2022). Rethinking carbon–neutral built environment: Urban dynamics and scenario analysis. *Energy and Buildings*, 255, 111672. https://doi.org/10.1016/j.enbuild.2021.111672
- Ikotun, A. M., Ezugwu, A. E., Abualigah, L., Abuhaija, B., & Heming, J. (2023). K-means clustering algorithms: A comprehensive review, variants analysis, and advances in the era of big data. *Information Sciences*, 622, 178–210. https://doi.org/10.1016/j.ins.2022.11.139
- Johnson, J., Brazier, C., & Lam, T. (2022). *The China Lab Guide to Megablock Urbanisms*. Actar D, Inc.
- Keirstead, J., Jennings, M., & Sivakumar, A. (2012). A review of urban energy system models: Approaches, challenges and opportunities. *Renewable and Sustainable Energy Reviews*, *16*(6), 3847–3866. https://doi.org/10.1016/j.rser.2012.02.047
- Li, D. H. W., & Wong, S. L. (2007). Daylighting and energy implications due to shading effects from nearby buildings. *Applied Energy*, 84(12), 1199–1209. https://doi.org/10.1016/j.apenergy.2007.04.005
- Liu, C., Sun, C., Li, G., Yang, W., & Wang, F. (2023). Numerical Simulation Analyses on Envelope Structures of Economic Passive Buildings in Severe Cold Region. *Buildings*, *13*(4), 1098. https://doi.org/10.3390/buildings13041098
- Liu, Z., Liu, Y., He, B.-J., Xu, W., Jin, G., & Zhang, X. (2019). Application and suitability analysis of the key technologies in nearly zero energy buildings in China. *Renewable and Sustainable Energy Reviews*, *101*, 329–345. https://doi.org/10.1016/j.rser.2018.11.023
- Long, Y., Li, P., & Hou, J. (2019). Three-dimensional urban form at the street block level for major cities in China. *Shanghai Urban Planning Review*, *3*(3), 10–15.
- Ma, M., Ma, X., Cai, W., & Cai, W. (2020). Low carbon roadmap of residential building sector in China: Historical mitigation and prospective peak. *Applied Energy*, 273, 115247. https://doi.org/10.1016/j.apenergy.2020.115247
- Ma, X., Wang, C., Dong, B., Gu, G., Chen, R., Li, Y., Zou, H., Zhang, W., & Li, Q. (2019). Carbon emissions from energy consumption in China: Its measurement and driving factors. *Science of The Total Environment*, *648*, 1411–1420. https://doi.org/10.1016/j.scitotenv.2018.08.183
- MoHURD. (202X). Technical standards for zero carbon buildings.
- Ng, M. K. (2002). Sustainable Urban Development Issues in Chinese Transitional Cities: Hong Kong and Shenzhen. *International Planning Studies*, 7(1), 7–36. https://doi.org/10.1080/13563470220112580
- Opel, O., Strodel, N., Werner, K., Geffken, J., Tribel, A., & Ruck, W. (2017). Climate-neutral and sustainable campus Leuphana University of Lueneburg. *Energy*, *141*, 2628–2639.
- Orehounig, K., Fierz, L., Allan, J., Eggimann, S., Vulic, N., & Bojarski, A. (2022). CESAR-P: A dynamic urban building energy simulationtool. *Journal of Open Source Software*, 7(78), 4261. https://doi.org/10.21105/joss.04261
- Pan, H., Zhuang, M., Geng, Y., Wu, F., & Dong, H. (2019). Emergy-based ecological footprint analysis for a mega-city: The dynamic changes of Shanghai. *Journal of Cleaner Production*, *210*, 552–562. https://doi.org/10.1016/j.jclepro.2018.11.064
- Shea, R. P., Worsham, M. O., Chiasson, A. D., Kelly Kissock, J., & McCall, B. J. (2020). A lifecycle cost analysis of transitioning to a fully-electrified, renewably powered, and carbon-neutral campus at

- the University of Dayton. *Sustainable Energy Technologies and Assessments*, 37, 100576. https://doi.org/10.1016/j.seta.2019.100576
- Su, C., Madani, H., & Palm, B. (2018). Heating solutions for residential buildings in China: Current status and future outlook. *Energy Conversion and Management*, *177*, 493–510. https://doi.org/10.1016/j.enconman.2018.10.005
- Valencia, A., Hossain, Md. U., & Chang, N.-B. (2022). Building energy retrofit simulation for exploring decarbonization pathways in a community-scale food-energy-water-waste nexus. *Sustainable Cities and Society*, 87, 104173. https://doi.org/10.1016/j.scs.2022.104173
- Venkatesh, A., Jaramillo, P., Griffin, W. M., & Matthews, H. S. (2011). Uncertainty in life cycle greenhouse gas emissions from United States natural gas end-uses and its effects on policy. *Environmental Science & Technology*, *45*(19), 8182–8189.
- Wang, H., Wu, H., Ding, Y., Feng, J., & Wang, S. (2015). Feasibility and optimization of aerogel glazing system for building energy efficiency in different climates. *International Journal of Low-Carbon Technologies*, 10(4), 412–419. https://doi.org/10.1093/ijlct/ctu010
- Wang, J., Huang, Y., Teng, Y., Yu, B., Wang, J., Zhang, H., & Duan, H. (2021). Can buildings sector achieve the carbon mitigation ambitious goal: Case study for a low-carbon demonstration city in China? *Environmental Impact Assessment Review*, *90*, 106633. https://doi.org/10.1016/j.eiar.2021.106633
- Wiryadinata, S., Morejohn, J., & Kornbluth, K. (2019). Pathways to carbon neutral energy systems at the University of California, Davis. *Renewable Energy*, *130*, 853–866. https://doi.org/10.1016/j.renene.2018.06.100
- Yang, X., Zhang, S., & Xu, W. (2019). Impact of zero energy buildings on medium-to-long term building energy consumption in China. *Energy Policy*, *129*, 574–586. https://doi.org/10.1016/j.en-pol.2019.02.025
- Yu, S., Eom, J., Zhou, Y., Evans, M., & Clarke, L. (2014). Scenarios of building energy demand for China with a detailed regional representation. *Energy*, 67, 284–297. https://doi.org/10.1016/j.energy.2013.12.072
- Zhang, L., Xia, J., Thorsen, J. E., Gudmundsson, O., Li, H., & Svendsen, S. (2016). Technical, economic and environmental investigation of using district heating to prepare domestic hot water in Chinese multi-storey buildings. *Energy*, *116*, 281–292. https://doi.org/10.1016/j.energy.2016.09.019
- Zhang, Q., Qiao, K., Hu, C., Su, P., Cheng, O., Yan, N., & Yan, L. (2024). Study on life-cycle carbon emission factors of electricity in China. *International Journal of Low-Carbon Technologies*, 19, 2287–2298. https://doi.org/10.1093/ijlct/ctae181
- Zhang, S.-C., Yang, X.-Y., Xu, W., & Fu, Y.-J. (2021). Contribution of nearly-zero energy buildings standards enforcement to achieve carbon neutral in urban area by 2060. *Advances in Climate Change Research*, *12*(5), 734–743. https://doi.org/10.1016/j.accre.2021.07.004
- Zheng, G., & Bu, W. (2018). Review of Heating Methods for Rural Houses in China. *Energies*, *11*(12), 3402. https://doi.org/10.3390/en11123402
- Zheng, H., Zhang, R., Yin, X., & Wu, J. (2025). Unused housing in urban China and its carbon emission impact. *Nature Communications*, *16*(1), 1985. https://doi.org/10.1038/s41467-025-57217-7
- Zhou, S., & Zhou, C. (2021). Evaluation of China's low-carbon city pilot policy: Evidence from 210 prefecture-level cities. *PLOS ONE*, *16*(10), e0258405. https://doi.org/10.1371/journal.pone.0258405







